CTH-RF-146 January 2000

Accelerator driven reactors

- the significance of the energy distribution of spallation neutrons on the neutron statistics

by

V. Fhager

CHALMERS UNIVERSITY OF TECHNOLOGY

DEPARTMENT OF REACTOR PHYSICS

ISSN 0281-9775

CTH-RF-146 January 2000

Accelerator driven reactors

- the significance of the energy distribution of spallation neutrons on the neutron statistics

by

V. Fhager

Master of Science degree thesis

Department of Reactor Physics
Chalmers University of Technology
S - 412 96 Göteborg, Sweden

This report is a degree thesis in Reactor Physics. It constitutes the final part of my M. Sc. education in engineering physics at *Chalmers University of Technology* in Göteborg, Sweden. The degree thesis is equivalent to 20 credit units, one credit unit representing at about one week's work.

The Department of Reactor Physics at Chalmers University was my host department for the thesis and the head of the department, Prof. Imre Pázsit, was my supervisor. It was started in June 1999 and completed in November the same year.

Although the task was given to me by the Department of Reactor Physics in Göteborg, the main part of the work was carried out at *Kyoto University Research Reactor Institute (KURRI)* in Kumatori, Japan.

Valentin Fhager

Göteborg, January 2000

Abstract

In order to make correct predictions of the second moment of statistical nuclear variables, such as the number of fissions and the number of thermalized neutrons, the dependence of the energy distribution of the source particles on their number should be considered. It has been pointed out recently that neglecting this number dependence in accelerator driven systems might result in bad estimates of the second moment, and this paper contains qualitative and quantitative estimates of the size of these errors.

We walk towards the requested results in two steps. First, models of the number dependent energy distributions of the neutrons that are ejected in the spallation reactions are constructed, both by simple assumptions and by extracting energy distributions of spallation neutrons from a high-energy particle transport code. Then, the second moment of nuclear variables in a sub-critical reactor, into which spallation neutrons are injected, is calculated. The results from second moment calculations using number dependent energy distributions for the source neutrons are compared to those where only the average energy distribution is used.

Two physical models are employed to simulate the neutron transport in the reactor. One is analytical, treating only slowing down of neutrons by elastic scattering in the core material. For this model, equations are written down and solved for the second moment of thermalized neutrons that include the distribution of energy of the spallation neutrons. The other model utilizes Monte Carlo methods for tracking the source neutrons as they travel inside the reactor material. Fast and thermal fission reactions are considered, as well as neutron capture and elastic scattering, and the second moment of the number of fissions, the number of neutrons that leaked out of the system, etc. are calculated. Both models use a cylindrical core with a homogenous mixture of core material.

Our results indicate that the number dependence of the energy distribution of the spallation neutrons leads to second moments that differ significantly from the ones calculated with the average energy distribution only. With the most realistic model of the energy distributions, the second moment of the number of fissions was underestimated with 12 - 16 %.

Sammanfattning

När man skall beräkna andra momentet, variansen, av statistiska fördelningar i en kärnreaktor, t.ex. antalet fissioner eller antalet utläckta neutroner, måste man ta hänsyn till att källneutronernas energifördelning kan bero på deras antal. Nyligen har man påpekat att om detta antalsberoende försummas när man studerar acceleratordrivna system kan det leda till att andra momentet beräknas felaktigt. Detta arbete innehåller kvalitativa och kvantitativa uppskattningar av hur stora dessa fel kan bli.

Arbetet sker i två steg. Först konstrueras modeller för hur spallationsneutronernas energifördelning beror på deras antal, både genom antaganden och genom att använda energispektra som beräknats med ett simuleringsprogram för partikeltransport vid höga energier. Sedan har andra momentet av vissa variabler beräknats då spallationsnetronerna skjutits in i en underkritisk reaktor. Resultatet från beräkningar med antalsberoende energifördelningar jämförs med beräkningar där bara ett medelspektrum har använts.

Två olika modeller har använts för att simulera neutroniken i reaktorn. Den ena är en analytisk modell som behandlar nedbromsning av neutroner genom elastisk spridning i reaktormaterialet. Explicita uttryck för andra momentet av antalet neutroner som bromsas till termisk energi sätts upp, där fördelningen av spallationsneutronernas energi ingår. Den andra modellen nyttjar Monte Carlo-metoder för att följa källneutronernas vandring i reaktorn. Där simuleras såväl snabb som termisk fission, liksom infångningsreaktioner och elastiska kollisioner. Andra momentet av antalet fissioner, antalet utläckta neutroner, m.m. beräknas. Båda modellerna inkluderar en cylindrisk reaktor med en homogen blandning av olika reaktormaterial.

Resultaten visar att beroendet av spallationsneutronernas energi på antalet neutroner gör att de beräknade andra momenten blir märkbart annorlunda mot om man bara skulle använda ett medelspektrum för deras energifördelning. Med den mest realistiska modellen för spallationsneutronernas energifördelning visar det sig att andra momentet av antalet fissioner skulle underskattas med 12 - 16 %.

Table of contents

1. Introduction

The background to the problems discussed in this paper is the following:

Neutron induced reactions in a fission reactor, such as fission and neutron scattering, are random processes. When neutron transport in a nuclear reactor is simulated, the main goal is to make correct predictions of the mean values of the quantities in question. For example, the average neutron flux in a number of points in the core is often sought for. But for thermal reactors, several theories and methods have been developed that also involve the second moment (the variance) of the neutron flux. For example, the *Feynman-alfa method,* which uses the second moment of the neutron flux to determine the reactivity, is one such method. Therefore, accurate calculation of the second moment is sometimes necessary.

In accelerator driven reactors, incident high-energy protons produce neutrons with energies up to hundreds of MeVs by spallation reactions in target nuclei. The neutrons will induce fission in fissile material that surrounds the target. However, in contrast to thermal reactors, the core will not be critical but can be operated in a subcritical mode since the spallation reactions act as an external source and thus provide the required neutron flux. This kind of reactor could be used for energy production, but applications of transmutation of spent nuclear fuel and as strong neutron sources have also been suggested.

Current methods of calculating the second moments of the neutron distribution in accelerator driven systems use the energy distribution of neutrons generated by a code that simulates the high-energy transport of particles inside the target. These neutrons are fed into a code that simulates the neutron transport in the lower energy range. All source neutrons are assumed to have the same energy distribution, independent of how many neutrons are generated in each spallation reaction. [1] This means that regardless of whether the number of spallation neutrons is 5 or 50, their average energy is always the same. The validity of this assumption is doubtful, considering the fact that the energy of the incoming particle is to be shared by the generated neutrons. In other words, neutrons that are born in a group of few neutrons others should be more energetic than neutrons that belong to a large-number group.

Picking the energy of a spallation neutron from an average spectrum regardless of the number of generated neutrons has no consequence for the calculation of mean values, but it might have a strong influence on the second and higher moments of calculated quantities.

If individual number dependent spectra do not differ much in appearance from the average spectrum, it might eventually be sufficient to use this latter only. This is for example the case in thermal fission, where it could not be excluded that different energy spectra exist for different numbers of fission neutrons. Nevertheless, the effect on higher moments is concluded to be negligible, mainly because the number of fission neutrons is small. [2]

For spallation systems however, where the number of generated neutrons might be as high as 80 and the neutron energies might exceed 1000 MeV, it is not hard to imagine

differences in energy spectra to be significant. It is thus an interesting question how big the differences are, what is their significance on the neutronics of the system, and quantitative estimates are called for.

Experimental data on the characteristics of such number dependent spectra do not exist today, and we are thus restricted to computer simulations for attacking the problem.

Some basic calculations on the influence of number dependent spectra, using very simple models, was carried out recently by Pázsit, Sjöstrand and Fhager [2]. The present work presents the results of extended calculations that were performed along the same lines. Considerably more realistic models of the spallation process and of the reactor itself are used, and the neutron transport simulation is based on Monte Carlo methods. But even if the models have been improved, the problem is still greatly simplified in this treatment, and many assumptions and simplifications have been made in order to make the problem possible to handle.

2. General principles

2.1 Distributions of spallation neutrons - some definitions

The number and energy distribution of the spallation neutrons is assumed to take the form

$$f(n, E) = p(n)\chi_n(E)$$

(eq. 2.1)

where $p(n)$ is the probability for n neutrons to be generated in a spallation event, and $\chi_n(E)dE$ is the probability for the neutrons to have energy E between E and $E + dE$. $\chi_n(E)$ is thus a probability density. [2]

Since $p(n)$ and $\chi_n(E)$ are probability distributions, they should be normalized to unity, so that

$$\sum_{n=0}^{\infty} p(n) = 1$$

(eq. 2.2)

and

$$\int_0^{\infty} \chi_n(E)dE = 1$$

(eq. 2.3)

The *average spectrum* is denoted $\bar{\chi}(E)$ and it is defined in the following way [2]:

$$\bar{\chi}(E) = \frac{\sum_{n=0}^{\infty} n \cdot p(n) \cdot \chi_n(E)}{\sum_{n=0}^{\infty} n \cdot p(n)} = \frac{1}{\bar{\nu}} \sum_{n=0}^{\infty} n \cdot p(n) \cdot \chi_n(E)$$

(eq. 2.4)

The average spectrum is thus built up by a sum of individual number dependent spectra, weighted with the n number of neutrons in each group, and with the probability of having n neutrons in a spallation event.

Since $p(n)$ and $\chi_n(E)$ are both normalized to unity, so is $\bar{\chi}(E)$, i.e.

$$\int_0^{\infty} \bar{\chi}(E)dE = \int_0^{\infty} \frac{1}{\bar{\nu}} \sum_{n=0}^{\infty} n \cdot p(n) \cdot \chi_n(E)dE = \frac{1}{\bar{\nu}} \sum_{n=0}^{\infty} n \cdot p(n) \cdot \underbrace{\int_0^{\infty} \chi_n(E)dE}_{=1} = \frac{\bar{\nu}}{\bar{\nu}} = 1$$

(eq. 2.5)

In (eq. 2.5) above, $\bar{\nu}$ denotes the *average number of spallation neutrons,* which may be as high as 30 or 40. This could be compared with thermal fission of e.g. ^{235}U, where the average number of fission neutrons is about 2.45.

The *average energy* $\bar{E}$ is defined as

$$\bar{E} = \int_0^{\infty} E \cdot \bar{\chi}(E)dE$$

(eq. 2.6)

and for neutrons generated by spallation with a 3 GeV proton, the mean energy may reach over 30 MeV, with individual neutrons gaining up to 2.5 GeV. This too, is quite different from thermal fission, where the mean energy of the generated neutrons is about 2 MeV and where individual neutrons rarely achieve energies above 10 MeV.

2.2 Analytical calculations of the number of thermalized neutrons

One approach to gain further understanding of how strongly the number dependent spectra of spallation neutrons affect the neutron statistics in a reactor is to study slowing down of source neutrons. By using first proper number dependent spectra for the spallation neutrons and calculating the distribution of neutrons slowing down to energy without leaking out, and then perform the same calculations assigning energies to the neutrons from an average spectrum, one can compare the two results and conclude if the difference is big or small. This approach allows writing down analytical expressions for the problem, which offers a clear and easy-to-grasp formulation, and makes computer

evaluation a straightforward task.

The significance of the energy distribution of source neutrons, such as spallation neutrons, becomes apparent when one tries to calculate statistic variables that involve integration with respect to energy. For example, the number of neutrons that slow down from initial energy to thermal energy without leaking out of the system can be written as a weighted integral, including an energy-dependent non-leakage probability. It will be shown below how the first and second moment of the distribution of slowed-down neutrons are calculated, and it will be pointed out how and where the energy distribution of the source neutrons enters the equations.

The first moment

The first moment - the mean value - of neutrons that slow down to thermal energy, denoted $\langle \nu \rangle$, can be written as a weighted integral

$$\langle \nu \rangle = \int_0^\infty P(E) \cdot p(E) dE \qquad \text{(eq. 2.7)}$$

where $P(E)$ is the non-leakage probability for a neutron with energy E, and $p(E)dE$ is the probability that after a spallation event, *one* neutron is in the energy interval dE at E [2].

$p(E)$ can be written, according to [2],

$$p(E) = \sum_{n=0}^{\infty} n \cdot p(n) \cdot \chi_n(E) \qquad \text{(eq. 2.8)}$$

or with use of (eq. 2.4),

$$p(E) = \bar{\nu} \cdot \frac{1}{\nu} \sum_{n=0}^{\infty} n \cdot p(n) \cdot \chi_n(E) = \bar{\nu} \cdot \bar{\chi}(E) \qquad \text{(eq. 2.9)}$$

The expression for $p(E)$ in (eq. 2.9) indicates that in order to calculate the first moment, only the average energy distribution of the source neutrons is needed. For the second moment the situation is different, which is shown in the following.

The second moment

In a way similar to the one above, the correct expression for the second moment of the number of thermalized neutrons, $\langle \nu(\nu-1)\rangle_{correct}$, is written

$$\langle \nu(\nu-1)\rangle_{correct} = \int_0^\infty \int_0^\infty P(E_1)\cdot P(E_2)\cdot p_{correct}(E_1, E_2)dE_1 dE_2$$

(eq. 2.10)

$p_{correct}(E_1, E_2)dE_1 dE_2$ is now the joint probability of finding one neutron in the energy interval dE_1 around E_1 and one in the interval dE_2 around E_2 [2].

The generalization of (eq. 2.9) in two dimensions reads ([2])

$$p_{correct}(E_1, E_2) = \sum_{n=0}^{\infty} n(n-1)p(n)\cdot \chi_n(E_1)\chi_n(E_2) = \langle n(n-1)\rangle \cdot \bar{\chi}(E_1, E_2)$$

(eq. 2.11)

$\bar{\chi}(E_1, E_2)$ is the two-point average energy distribution, defined as

$$\bar{\chi}(E_1, E_2) = \frac{\sum_{n=0} n(n-1)p(n)\cdot \chi_n(E_1)\chi_n(E_2)}{\langle n(n-1)\rangle}$$

(eq. 2.12)

and

$$\langle n(n-1)\rangle = \sum_{n=0}^{\infty} n(n-1)p(n)$$

(eq. 2.13)

is the second moment of the number of generated spallation neutrons.

There is no way the sum of individual energy distributions $\chi_n(E)$ in (eq. 2.11) can be replaced by the average one-point distribution $\bar{\chi}(E)$, which is the case in (eq. 2.8). Knowledge of the number dependent spectra $\chi_n(E)$, or at least the weighted sum in (eq. 2.11), is thus a condition for calculating the second moment.

If one yet wants to replace $\chi_n(E)$ with $\bar{\chi}(E)$ in the expression for $p(E_1, E_2)$ above, which is the same as saying that the average spectrum describes the energy distribution of all neutron groups and that there is no dependence on the number of generated neutrons, an "average" expression for the second moment is obtained ([2]):

$$\langle \nu(\nu-1)\rangle_{average} = \int_0^\infty \int_0^\infty P(E_1)\cdot P(E_2)\cdot p_{average}(E_1, E_2)dE_1 dE_2$$

(eq. 2.14)

where

$$p_{average}(E_1, E_2) = \sum_{n=0}^{\infty} n(n-1)p(n) \cdot \bar{\chi}(E_1) \cdot \bar{\chi}(E_2) = \langle n(n-1) \rangle \cdot \bar{\chi}(E_1) \cdot \bar{\chi}(E_2)$$

(eq. 2.15)

The ratio

$$\alpha = \frac{\langle \nu(\nu-1) \rangle_{correct}}{\langle \nu(\nu-1) \rangle_{average}} = \frac{\int_0^\infty \int_0^\infty P(E_1) \cdot P(E_2) \cdot \bar{\chi}(E_1, E_2) dE_1 dE_2}{\int_0^\infty \int_0^\infty P(E_1) \cdot P(E_2) \cdot \bar{\chi}(E_1) \cdot \bar{\chi}(E_2) dE_1 dE_2}$$

(eq. 2.16)

indicates how strongly the number dependence of the spallation neutron spectra affects the second moment calculations of thermalized neutrons.

The *correlation function* $c(E_1, E_2)$ is defined as

$$c(E_1, E_2) = \bar{\chi}(E_1, E_2) - \bar{\chi}(E_1) \cdot \bar{\chi}(E_2)$$

(eq. 2.17)

and this too serves as an indicator on the strength of the number dependence. This function is non-zero when two or more neutrons are correlated, which is the case in spallation events, where several neutrons are simultaneously generated. [2]

If, for all n, $\chi_n(E)$ would be equal to $\bar{\chi}(E)$, the correlation function $c(E_1, E_2)$ would be zero.

It is clear from the above that energy distributions of individual groups of source neutrons must be known if the second moment of the number of slowed-down neutrons is to be determined. This also holds for other statistical numbers that involves energy dependence, e.g. the second moment of the number of fissions in the core.

Therefore, the goal of this paper is two-fold:

1. To generate realistic number dependent energy distributions

2. Given these distributions, calculate the second moment of some statistical variables. The results are then to be compared with what would come out from calculations that use only the average energy distribution.

In part one, models of energy spectra are constructed both from simple models of how the spallation energy is distributed among the generated particles, and from energy distributions that have been calculated by an established code for spallation simulation.

In part two, second moments are calculated with two different techniques. One is to treat the problem of neutron slowing-down in a homogenous reactor where the source neutrons are assumed to be generated everywhere in the core volume, and where elastic neutron scattering is assumed to be the dominating nuclear reaction. An energy-dependent non-leakage probability is calculated from *Fermi age theory*, and the expressions for the second moment in the above are explicitly evaluated. The second approach is to use *Monte Carlo simulation* of the neutron transport in the reactor. The reactor materials are still considered to be homogeneously distributed in the core, but spallation neutrons are locally injected, and nuclear reactions other than just inelastic scattering are taken into consideration.

Spallation spectrum models are presented in chapter 3.4, and the results from the two ways of calculating second moments by using these models are presented in chapter 4.1.3 and 4.2.4 respectively.

3. Calculating number dependent spallation spectra

3.1 The spallation process

The spallation process concerns the thermal excitation of heavy nuclei with charged particles, usually protons, and the subsequent de-excitation of these nuclei by ejection of particles and quanta. For purposes of accelerator driven systems, neutrons are the most interesting of the ejected particles [3]. The ejection of neutrons and protons that follow from excitation of a target nucleus can be divided into two main steps:

1) Inter-nuclear collision cascades
2) Evaporation during de-excitation of the nucleus

Figure 1 below illustrates the two steps of the spallation process.

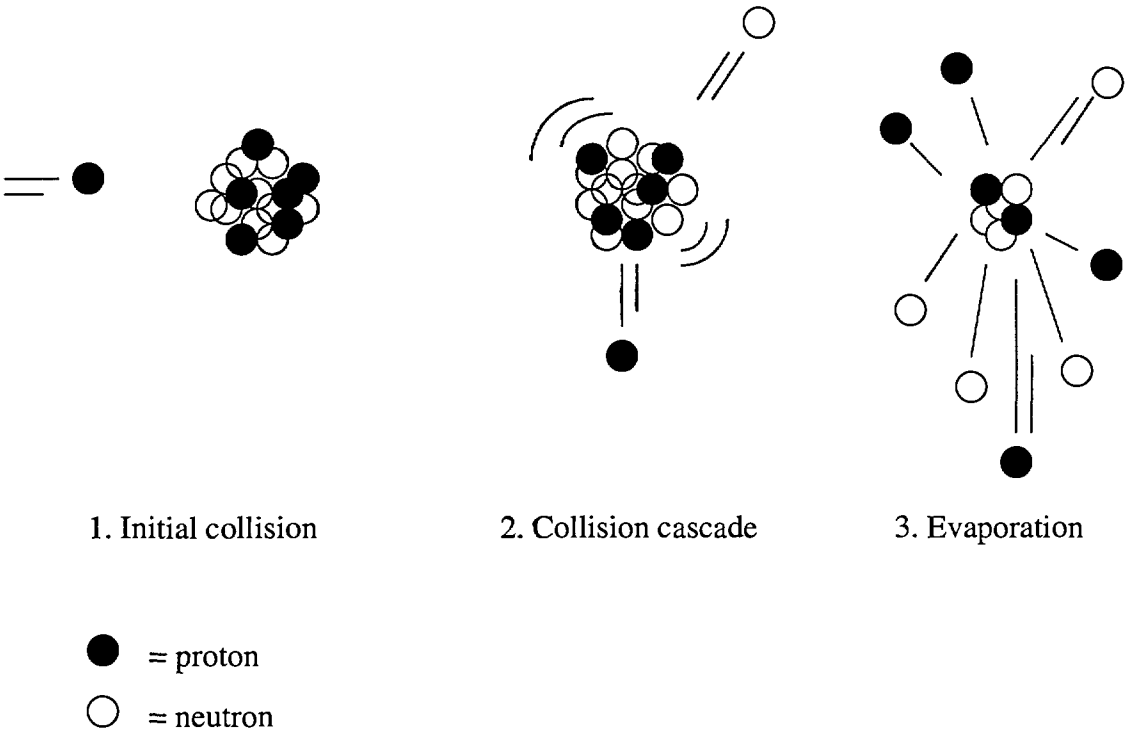

FIGURE 1. The spallation process.

In steps one and two, the incoming particle (the proton) collides with some of the nucleons in the target nucleus. The nucleons cause additional collisions in their turn, and in the cascade of collisions established, some of the nucleons gain enough energy to leave the nucleus. The energy of these nucleons can be very high, but only a minor part of the particles released in a spallation reaction leave the target nucleus this way. Most nucleons are instead ejected in step three. A large fraction of the energy of the incoming particle that was transmitted to the nucleus through violent internuclear collisions will put the nucleus in an excited state. It then de-excites into a more stable state of lower energy by ejecting neutrons, protons and other particles, and also gamma radiation. The situation is similar to evaporation of water molecules from a hot surface.

The energy of the "evaporation" neutrons and protons is quite low, only a few MeV on average, which is much lower than the energies of nucleons ejected in collision cascades. And since evaporation of neutrons from the excited nucleus is the dominating ejection mechanism, low energy neutrons dominate the total spectrum of spallation neutrons, as demonstrated in Figure 2. The plot in this figure was fitted to an energy distribution that was calculated by Dr. Hilscher at HMI Institute in Berlin, using a high-energy particle transport code to simulate the transport of spallation neutrons in a cylindrical lead target [3].

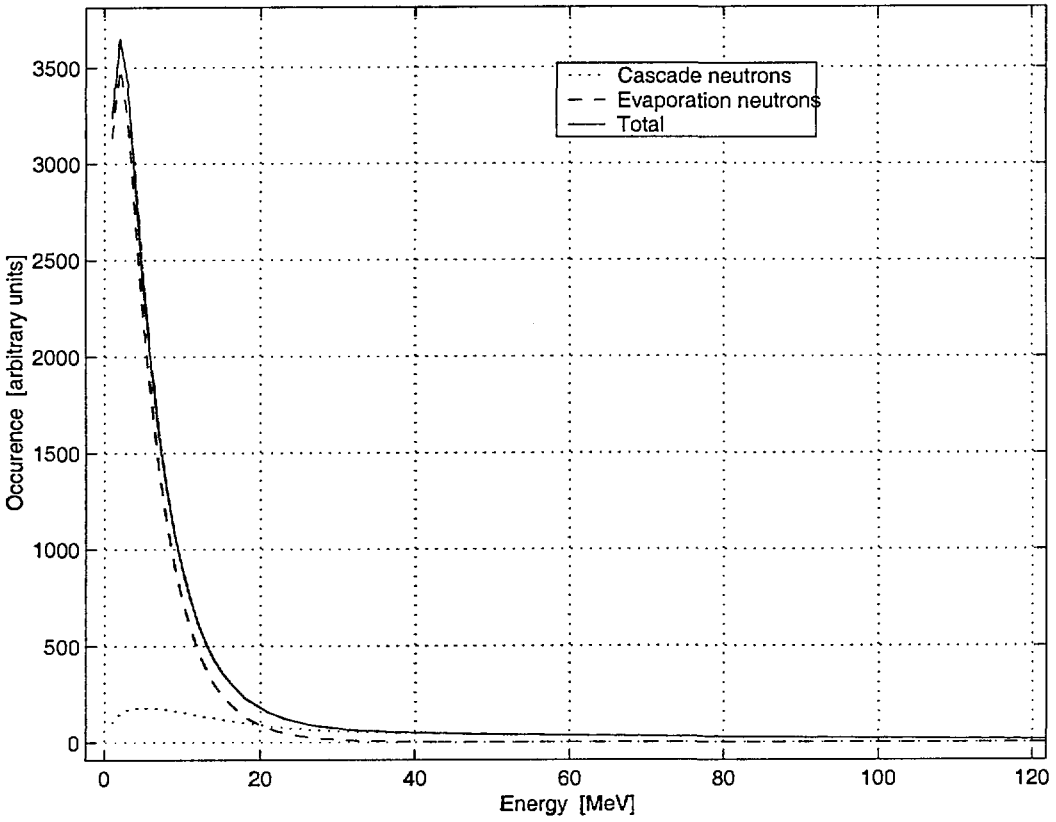

FIGURE 2. Energy distribution of spallation neutrons ejected through collision cascades and evaporation.

3.2 A spallation model

In order to simulate the influence of number dependent spectra of spallation neutrons on the neutron statistics, a concrete form of the number dependence must be prepared. As a first step, a model for relating the average neutron energy to the number of spallation neutrons is developed. In this spallation model, it is assumed that the average energy of a neutron that originates from a spallation event where a certain number of neutrons are released is:

$$E_n = \eta_{sp} \cdot \frac{E_p - (n+p) \cdot E_B}{n+p} \qquad \text{(eq. 3.1)}$$

where

n = number of neutrons from one spallation event
p = number of protons from one spallation event
E_n = average neutron energy in a group with n spallation neutrons
E_p = energy of the incoming particle (proton)
E_B = binding energy of one nucleon in the target nucleus
η_{sp} = fraction of the available energy that is transmitted to the nucleons in the spallation.

The incident particle carries a kinetic energy E_p which is distributed among the spallation products, such as nucleons and rest fragments of the target nucleus.

A part of the incoming kinetic energy of the proton is needed to release the nucleons from the nucleus, to which they are bound with a binding energy E_B, for both neutrons and protons. This reduces the available kinetic energy to $E_p - (n+p) \cdot E_B$.

The fact that a fraction of the energy is lost to rest fragments, and also gamma radiation, is taken into account in this model by introducing the efficiency coefficient η_{sp}, which is between 0 and 1.

Throughout this work, the target material is ^{208}Pb, and it has been assumed that the number of ejected protons p, is proportional to the number of ejected neutrons n, in the same way as the number of protons and neutrons are related in the ^{208}Pb nucleus, i.e.

$$\frac{p}{n} = \frac{82}{126}$$

(eq. 3.2)

which leads to (eq. 3.3)

$$E_n = \eta_{sp} \cdot \frac{E_p - n \cdot \left(1 + \frac{126}{82}\right) \cdot E_B}{n \cdot \left(1 + \frac{126}{82}\right)}$$

(eq. 3.3)

The assumed relation in (eq. 3.2) is a quite bad approximation of the actual ratio of the number of protons and neutrons, which has been found to be at about 1/10 or less, due to the higher binding energy of the proton, but it will be sufficient for this model.

The validity of (eq. 3.3) has been investigated by comparison with the average energy of spallation neutrons calculated with the spallation simulation code *NMTC/JAERI97* described below.

3.3 *NMTC/JAERI97* calculations

The nucleon meson transport code *NMTC/JAERI97* was developed by *Japan Atomic Energy Research Institute (JAERI)* for studying nuclear spallation reactions and particle transport in a medium. The code can simulate both the primary spallation reaction and the secondary particle transport in the intermediate energy region from 20 MeV to 3.5 GeV by the use of the Monte Carlo technique [4].

The incident particle in the spallation reaction can be either a nucleon or a pion whose upper energy limits are 3500 MeV and 2500 MeV respectively.

Some of the output that can be obtained from the code are:

- a list of neutrons, with energy below a certain level, recorded with their positions and velocities
- the neutron flux at the target boundaries
- the number of intra-nuclear collisions, spallation reactions, neutron captures etc.
- the nuclide yield of a number of isotopes produced in the target

In this work, *NMTC/JAERI97* has been used to determine the number distribution and energy distributions of spallation neutrons that follow from simulations of the spallation process.

The distributions were extracted from *NMTC/JAERI97* by setting a certain parameter to 3000 MeV, which was equal to the energy of the incoming proton.With this setting, all neutrons that are born with energies less than 3000 MeV are registered by their energy and position and then taken out of the system, prevented from causing any secondary nuclear reaction. Therefore, all *NMTC/JAERI97* spectra presented here describe the distribution of *primary* spallation neutrons, which means that the neutrons have not yet interacted with the surrounding material [4].

3.3.1 The spallation neutron number distribution

To extract the number distribution of spallation neutrons from *NMTC/JAERI97* calculations, the number of generated neutrons was counted in 10 000 spallation events, each with a 3 000 MeV proton striking a lead target. A sharp peak is observed in the distribution for very low values of n and negligible probability for $n > 65$.

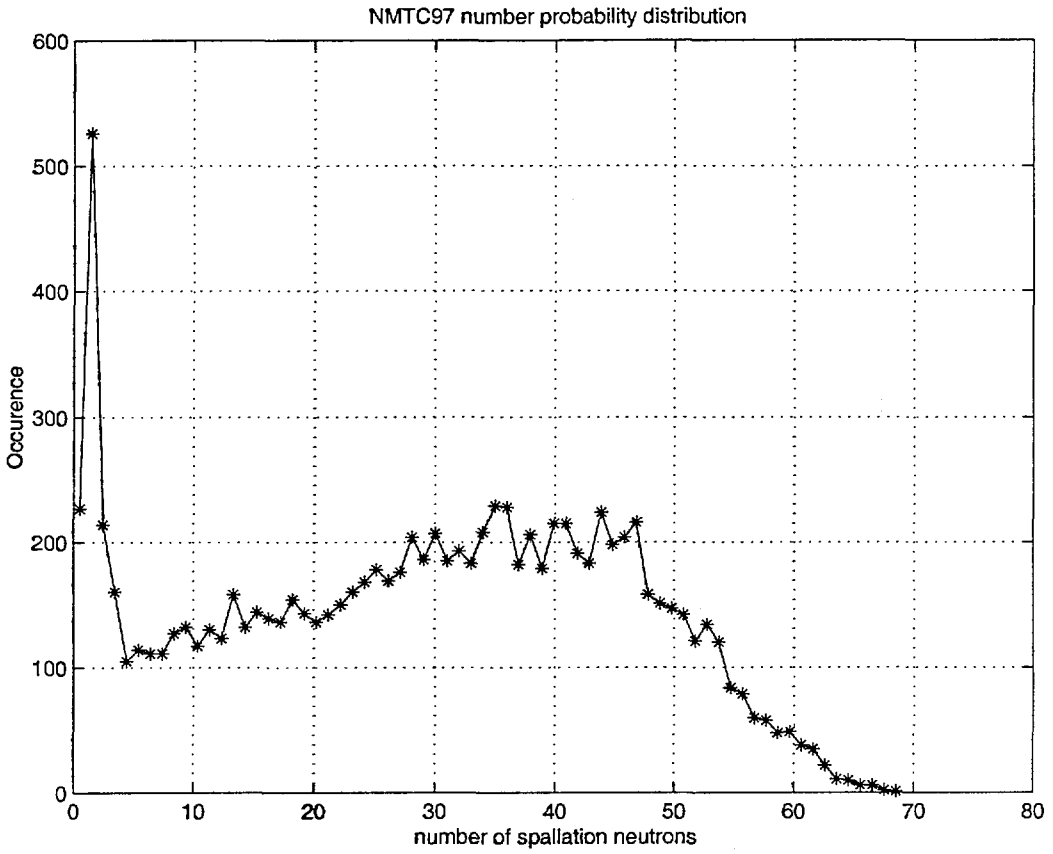

FIGURE 3. Number distribution of spallation neutrons calculated in a *NMTC/JAERI97* simulation where the proton energy was 3000 MeV.

The average neutron number ($\bar{\nu}$) is 30.0 for this distribution.

The probability distribution plotted in Figure 3 reproduces the main features of a similar probability distribution that has been calculated by Hilscher et al. [5]. Compared to those results, *NMTC/JAERI97* produces a number probability distribution with a somewhat sharper peak at low n, and a bit lower average number of neutrons.

When calculating the second moments according to the equations in chapter 2.2, the distribution plotted in Figure 3 was used to model the probability of the number of spallation neutrons.

3.3.2 Energy spectra of spallation neutrons

We used the code *NMTC/JAERI97* to calculate energy spectra for the numbers of spallation neutrons between 1 and 65. Plots of these spectra are presented in Figure 4.

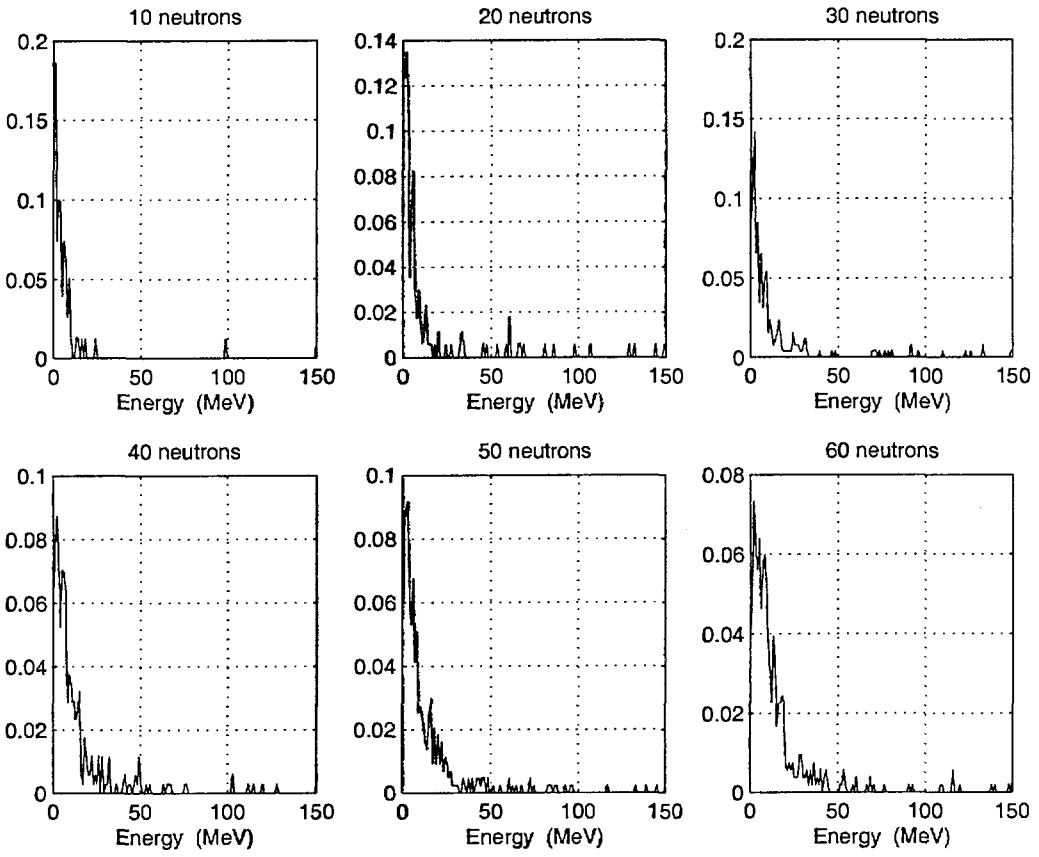

FIGURE 4. Energy distributions for various groups of spallation neutrons, calculated in a *NMTC/JAERI97* simulation where the proton energy was 3000 MeV.

The non-smooth character of the plotted spectra is due to poor statistics. For each neutron number n between 1 and 65, the energy of the neutrons from 100 spallations (in which n neutrons are produced) is sampled. Thus, in the case of $n = 50$, the number of neutrons contributing to the spectrum is $50 \times 100 = 5000$, which is quite reasonable. But for the cases where the number of neutrons is small, the spectra will be built-up by very few energy values. However, these spectra serve mainly as indications on what the individual number dependent spectra will look like, and details of the spectra need not to be in the focus of interest.

As can be seen in Figure 4, most spectra look very much the same, independent of the number of neutrons. Low energies are dominating and only a small fraction of the neutrons have energies over 20 MeV. However, the average energy of each group of neutrons was calculated, and it varies considerably, which is indicated in Figure 5.

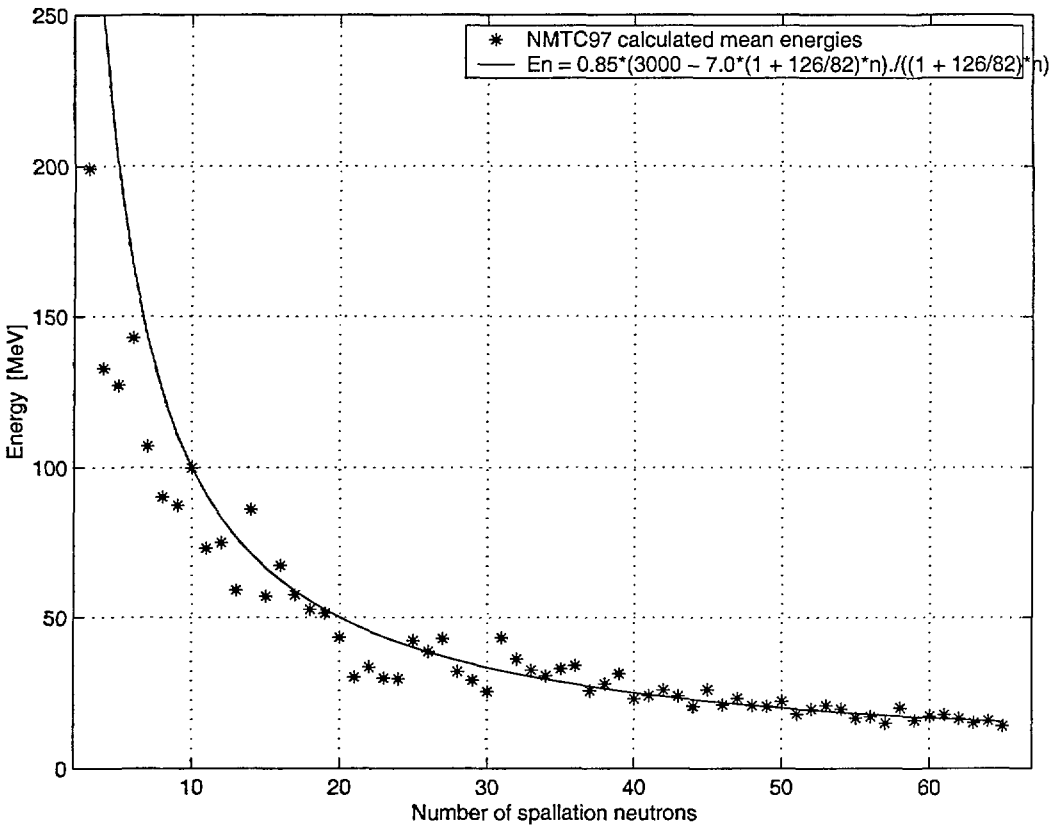

FIGURE 5. Average energies for different groups of spallation neutrons, calculated with *NMTC/JAERI97* and with (eq. 3.1).

In Figure 5, a curve has been included that shows the average energies predicted by the formula (eq. 3.1). When E_B is set to 7 MeV in the equation, and η_{sp} is set to 0.85 for a case where E_p = 3000 MeV, good agreement between the E_n:s predicted by (eq. 3.1) and the average energies calculated with *NMTC/JAERI97* is obtained.

As mentioned above, the spectra plotted in Figure 4 represent the energy distributions of *primary* neutrons, which means that the neutrons could be thought of as coming from a very thin target. In most realistic cases, a thick target will be used. In thick targets, primary spallation neutrons and protons will induce secondary neutrons in intra-nuclear cascades. Secondary neutrons produced in such reactions will of course have lower energy than the primary ones, and thus the energy distribution of neutrons that leave a thick target will be pushed even further to the low-energy region, compared to the spectra of primary neutrons. An important result will be that the small differences in spectra, due to different numbers of primary spallation neutrons, will be decreased further during the following intra-nuclear cascades. This fact, together with the similarities between individual spectra in Figure 4 give reasons to believe that for most practical applications of accelerator driven systems where macroscopic spallation targets are used, the effects of number dependent energy spectra on the variation of the number of nuclear reactions in an adjoining core are small. However, this will be investigated quantitatively in the following.

3.4 Spectrum models

With (eq. 3.1), we have a formula that provides us with the average energy of each neutron group, and we turn to the next problem:
How is the energy of each neutron group distributed around the average energy?

The answer could of course be found in the energy spectra that has already been extracted from *NMTC/JAERI97* calculations (Figure 4). Creating spectrum models that resemble these distributions and using them for calculating second moments would surely yield the most realistic results. However, it is also interesting to know how strongly the second moment calculations depend on the source neutrons in general, and we find it suitable to also include some other spectrum models. These models must not necessarily be fully realistic, but instead exaggerate the number dependence, so that the energy distribution of each group of neutrons differ considerably from the average spectrum.

The three different spectrum models that have been developed in this paper are as follows:

1. Gaussian distribution
2. Maxwell distribution
3. Piece-wise linear distribution

1. Gaussian distribution

A very simple model of the distribution of neutron energy would be to assume that all neutrons belonging to a group of n neutrons have the same energy E_n.
The energy distribution is then described by a *Dirac delta function:*

$$\chi_n(E) = \delta(E - E_n)$$

(eq. 3.4)

It is of course completely unrealistic to assume that all neutrons are ejected with exactly the same energy, but we keep this spectrum model for the purpose of comparison. It serves as a valuable extreme case where the number dependence is strongly exaggerated.

Instead of using exact Dirac delta functions, Gaussian distributions of the spallation neutron energy are employed:

$$\chi_n(E) = \frac{1}{\sigma\sqrt{2\pi}} e^{-\frac{1}{2}\left(\frac{E-E_n}{\sigma}\right)^2}$$

(eq. 3.5)

Here, E_n is the average energy for a group of n neutrons, and σ is the *standard deviation* (in energy units) of the distribution. By changing the parameter σ, one can vary the "sharpness" of the distribution, resulting in a very broad spectrum if σ is large.
If instead σ is small, the Gaussian distribution will be a sharp peak, centred around E_n, and in the limit when $\sigma \to 0$, it becomes indeed a Dirac delta function:

$$\lim_{\sigma \to 0} \frac{1}{\sigma\sqrt{2\pi}} e^{-\frac{1}{2}\left(\frac{E-E_n}{\sigma}\right)^2} = \delta(E-E_n)$$

(eq. 3.6)

Figure 6 shows Gaussian distributions for some different n, along with the average spectrum $\chi(E)$, as calculated from (eq. 2.4), using (eq. 3.5) for $\chi_n(E)$.

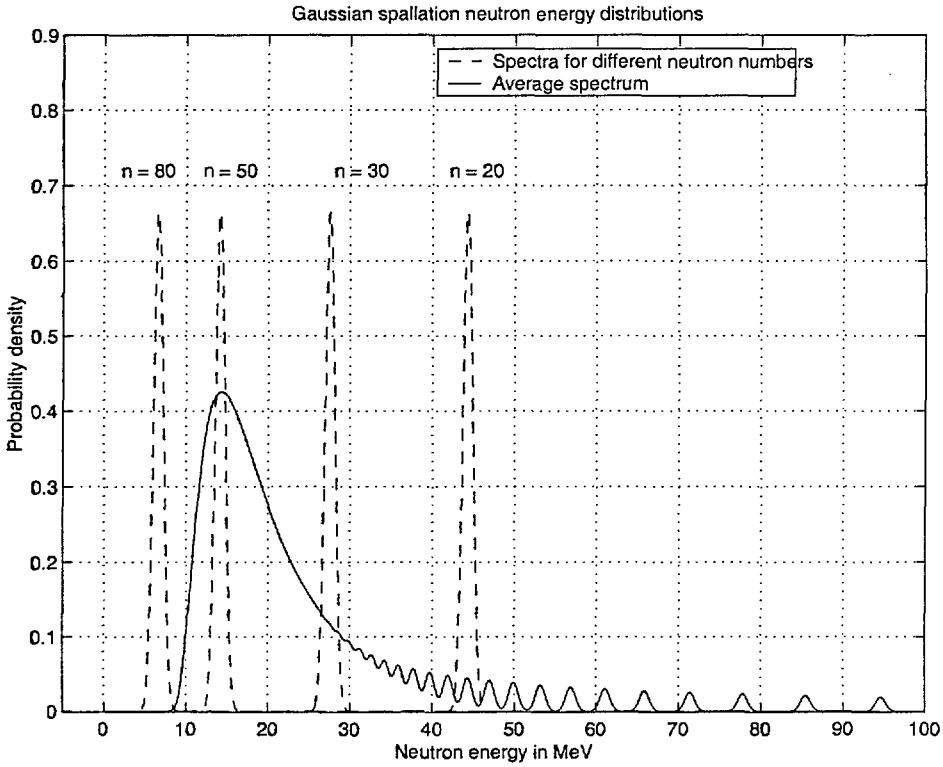

FIGURE 6. Some number dependent spectra and the average spectrum of spallation neutrons with Gaussian energy distribution. A standard deviation of σ = 0.6 MeV was used.

The two-dimensional correlation function, defined by (eq. 2.15), corresponding to a Gaussian distribution is shown in Figure 7. Here, a value of σ = 0.6 MeV was used.

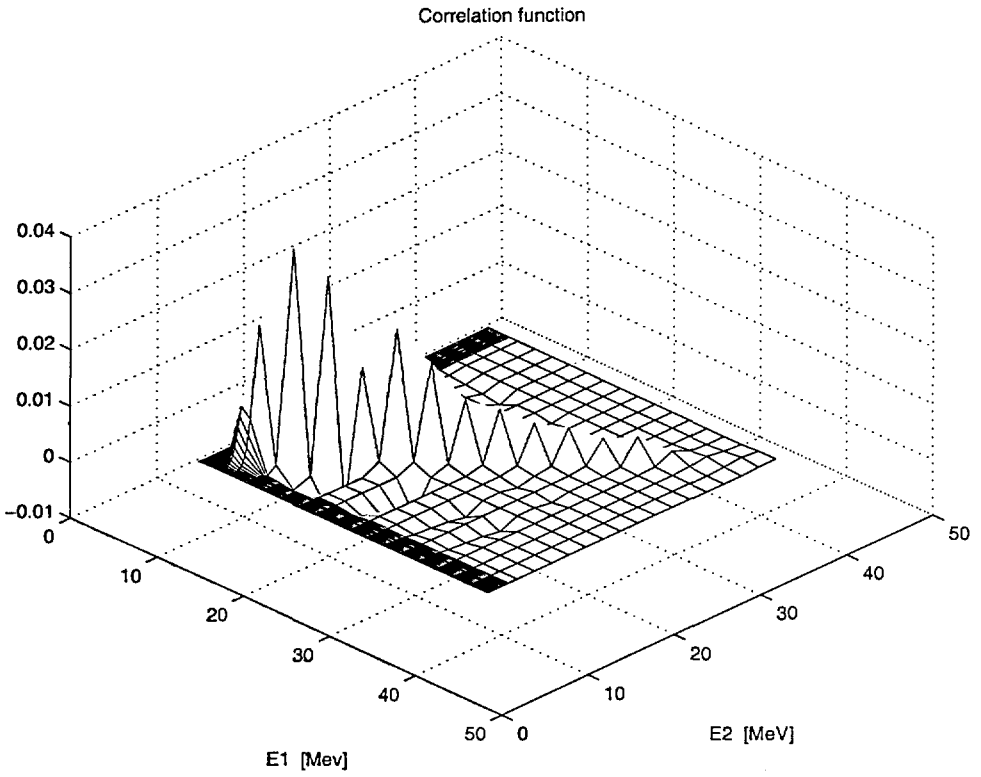

FIGURE 7. Two-dimensional correlation function of a Gaussian spectrum model where a standard deviation of σ = 0.6 MeV was used.

2. Maxwell distribution

A Maxwell distribution of the energy of the spallation neutrons would define the number dependent spectra $\chi_n(E)$ according to

$$\chi_n(E) = \frac{4E}{E_n^2} e^{-\frac{2E}{E_n}} \qquad \text{(eq. 3.7)}$$

where E_n is the average energy for a group of n neutrons, which would also be the average energy of the Maxwell distribution.

If no information were given on what the real energy distribution of the spallation neutrons is like, a Maxwell distribution would be a clever guess. This particular distribution appears frequently in the fields of statistical physics and thermodynamics. De-excitation of a nucleus shows similarities to the process of molecules evaporating from a hot surface - encouraging facts to those who suggest a Maxwell distribution to describe the energy spectra of spallation neutrons.

Furthermore, a Maxwell distribution is a quite good approximation of fission neutron spectra, which is illustrated in Figure 8. If spallation and thermal fission had any common features in the process of ejecting neutrons, it would not be a bad guess that Maxwell distributions be a fairly good approximation of the energy spectra of spallation

neutrons.

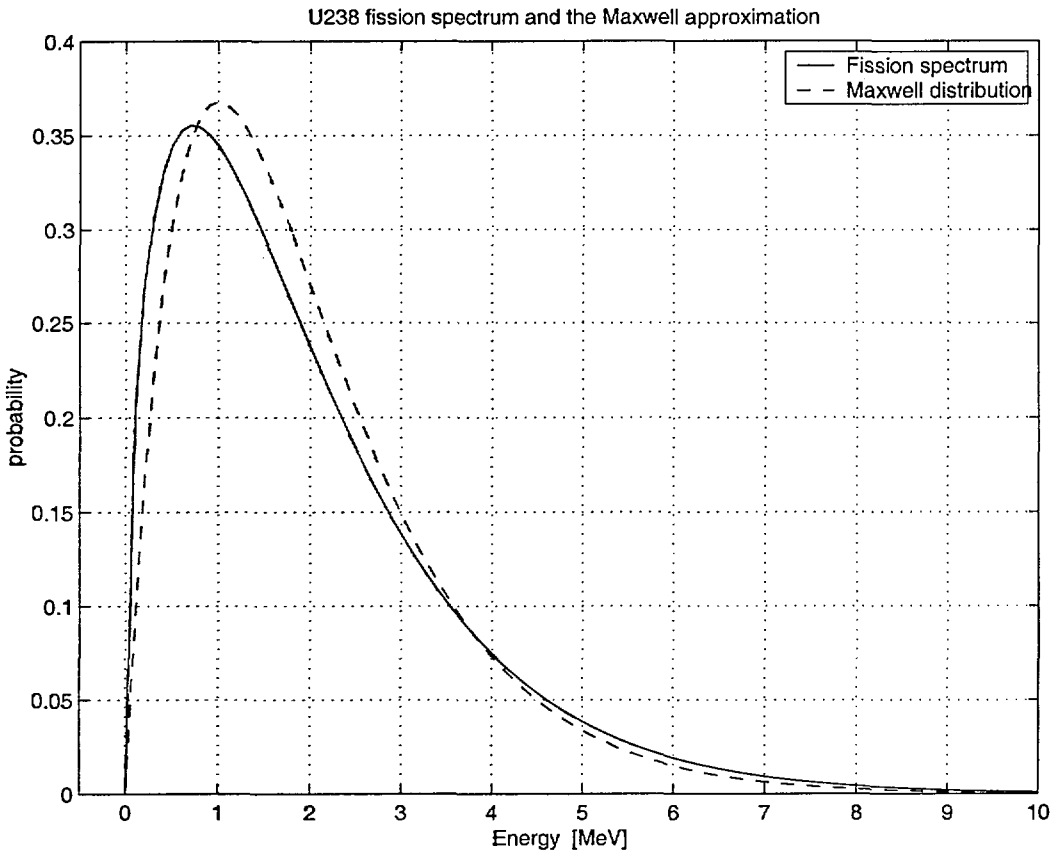

FIGURE 8. The energy distribution of neutrons generated in thermal fission of ^{235}U and a Maxwell distribution that approximates the fission spectrum.

Maxwell distributions for different n are plotted together with the average spectrum $\bar{\chi}(E)$ in Figure 9, and the correlation function is plotted in Figure 10.

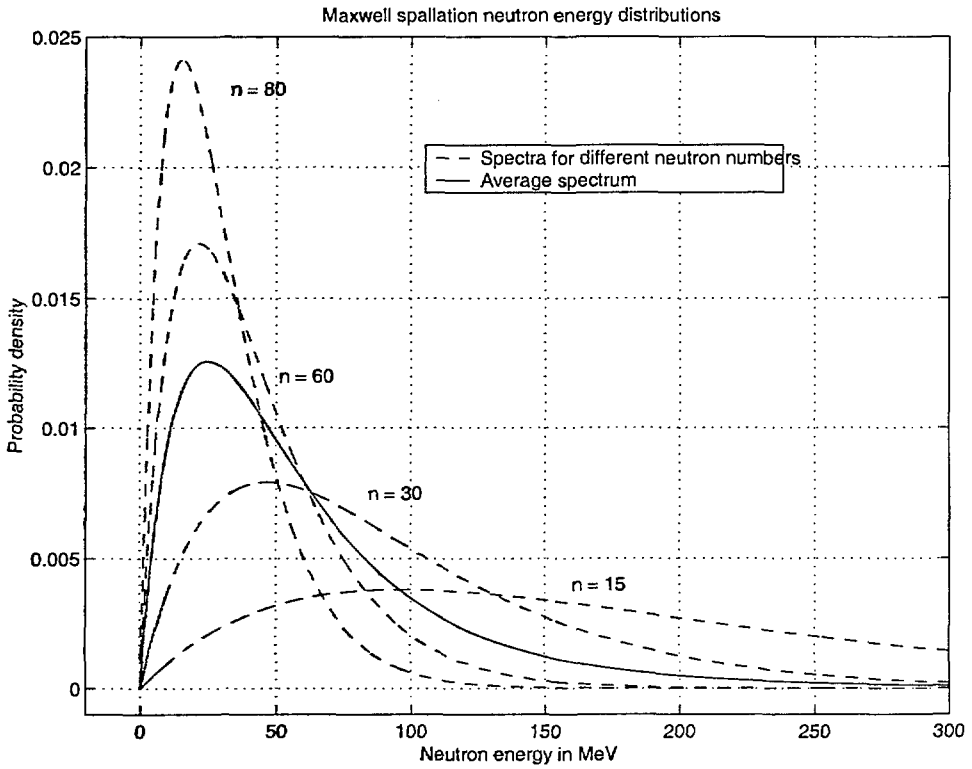

FIGURE 9. Some number dependent spectra and the average spectrum of spallation neutrons with Maxwell energy distribution.

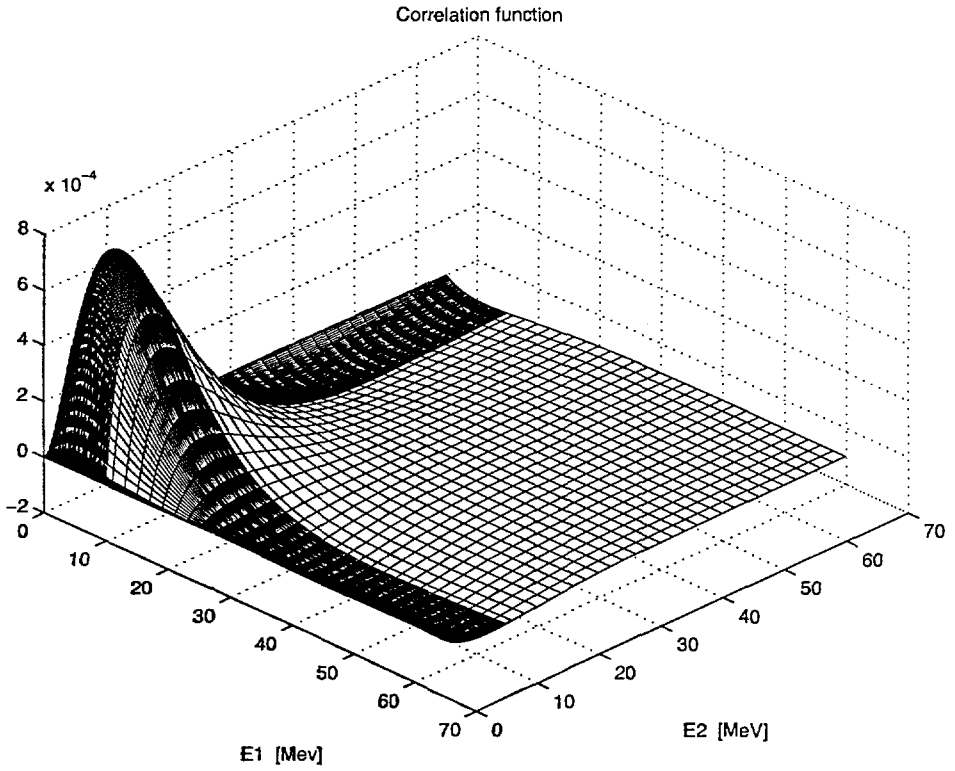

FIGURE 10. Two-dimensional correlation function of a Gaussian spectrum model.

3. Piece-wise linear distribution

In order to model the number dependent spectra that has been extracted from *NMTC/ JAERI97* simulations, a piece-wise linear distribution of the neutron energy has been constructed. This spectrum model consists of two linear parts, each defined on the two intervals $[0, E_2]$ and $[E_2, E_{max}]$. E_{max} is the highest energy that a spallation neutron can achieve, which is set equal to the energy of the incoming bombarding particle. E_2 is a break-point energy that varies with the number of spallation neutrons n. Good agreement between the model and the spectra that has been extracted from *NMTC/ JAERI97* is achieved by varying the *break-point energy* E_2 linearly from 8 MeV for n = 5 to 22 MeV for n = 65.

The dominance of low-energy neutrons that is so significant in the *NMTC/JAERI97* spectra is kept in the linear model, the major part of the neutrons belonging to the energy interval $[0, E_2]$. In Figure 11, where some of the distributions are plotted, it looks like the probability function becomes zero when the energy exceeds the break-point energy E_2, but this is only due to the very small slope of the straight line in this energy region. The tiny fraction of neutrons that belong to the upper interval merely serve as adjustments of the average energy.

When the piece-wise linear spectrum model is constructed, two parameters, p_1 and p_2 are used to define the break-points of the distribution together with E_2 and E_{max}. They are the probability densities at $E = 0$ and at $E = E_2$. The value of these two parameters is determined by the normalization condition

$$\int_0^\infty \chi_n(E)dE = 1 \qquad \text{(eq. 3.8)}$$

and by demanding the average energy to be equal to E_n:

$$\bar{E}(n) = \int_0^\infty E \cdot \chi_n(E)dE = E_n \qquad \text{(eq. 3.9)}$$

Some piece-wise linear spectra and the correlation function are shown in Figure 11 and Figure 12 below.

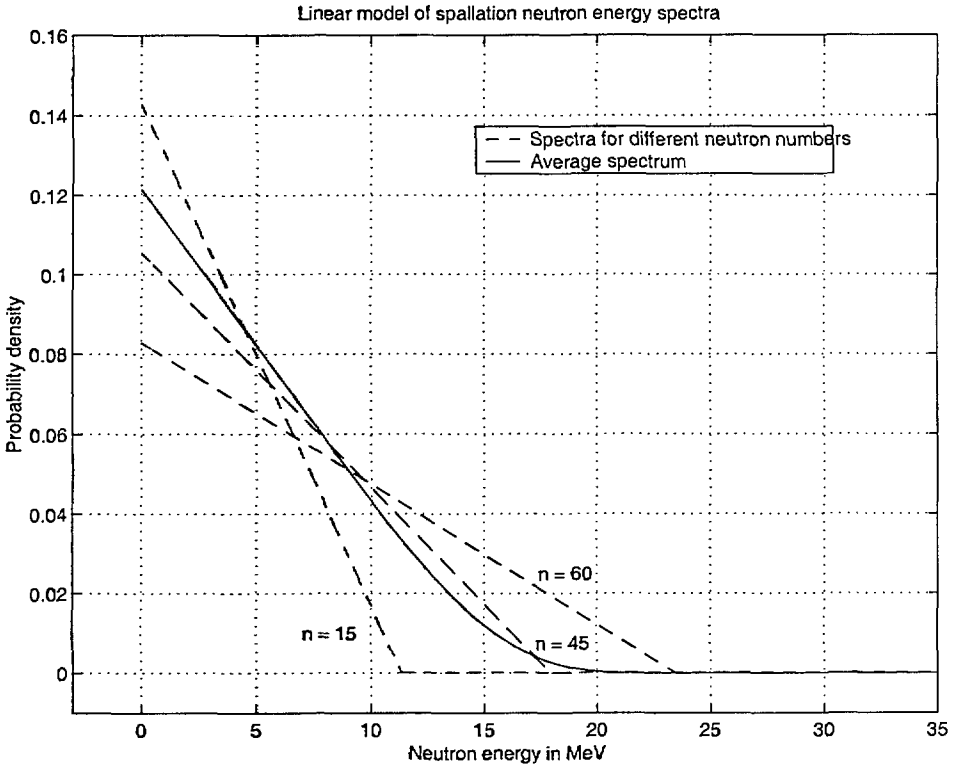

FIGURE 11. Some number dependent spectra and the average spectrum of spallation neutrons with a piece-wise linear energy distribution, modelling spectra that were calculated by *NMTC/JAERI97* for a case where the proton energy was 3000 MeV.

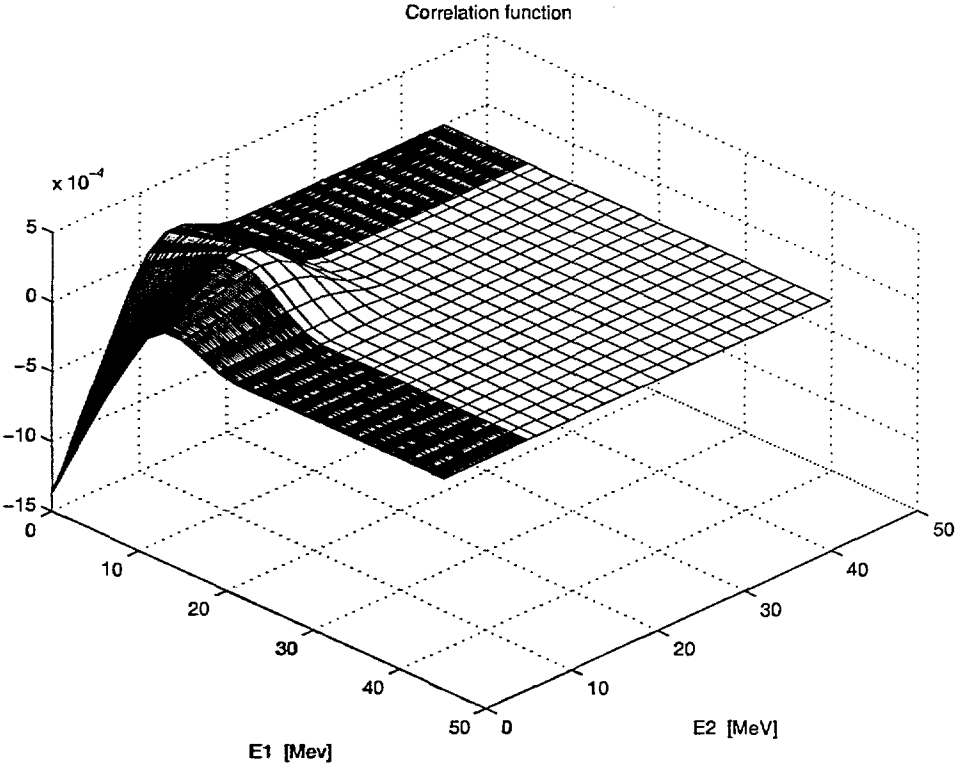

FIGURE 12. Two-dimensional correlation function of a piece-wise linear spectrum model.

All three spectrum models presented here have been used for calculating the second moment of some statistical distributions of variables in a nuclear reactor, into which source neutrons with such energy distributions have been injected.

As one would expect, it turns out that the difference between calculating the second moment with number dependent spectra and doing the same calculations using only the average spectrum is most prominent with Dirac delta functions and almost vanishing with the piece-wise linear model.

The various approaches for calculating the second moment in this work, and the details of the calculations and computer programs that have been developed and used are presented in the following chapter.

4. Calculating the second moment

In the previous chapter, a number of models for the distribution of the energy of spallation neutrons was elaborated. Here, we will focus on the calculations of second moments using these spectrum models.
We start with a treatment of the process of slowing-down of neutrons, following the ideas in chapter 2.2, and we make use of Fermi age theory to enable evaluation of the expressions stated there.
Next, we employ Monte Carlo techniques for simulating the neutron transport, which helps us to calculate the second moments of several variables, e. g. the number of fissions and the number of out-leaked neutrons.

4.1 Fermi age theory

The Italian physicist Enrico Fermi first presented his theory on slowing-down of neutrons in a thermal reactor due to elastic scattering in the 1940s. In this paper, only a few concepts of the theory are presented, just enough to write down a simple expression for the non-leakage probability of reactor neutrons.
A more detailed presentation of the Fermi age theory is given for example in [6].

Fermi introduced the concept of age for thermal neutrons with a certain source energy, according to

$$\tau(E) = \int_{E_{th}}^{E} \frac{l_{tr} l_s}{3\xi} \cdot \frac{dE'}{E'}$$

(eq. 4.1)

where l_{tr} and l_s are *the transport mean free path* and *the scattering mean free path* respectively, and ξ is the *average increase of lethargy per collision* [7].

The age increases with the size of the energy interval $E - E_{th}$, so that a neutron that is slowed down from energy E to E_{th} is "older", i.e. has higher age, the larger the energy interval $E - E_{th}$ is.

With this definition, Fermi was able to derive a simple expression for the *non-leakage probability* $P(E)$ for neutrons with energy E:

$$P(E) = e^{-B^2\tau(E)} \qquad \text{(eq. 4.2)}$$

where B^2 is the *geometrical buckling* of the reactor [7].

The validity of Fermi age theory is restricted to reactors where the neutrons interact with the core material by elastic scattering only, and where the spatial and energy dependence can be separated.

The expression of the non-leakage probability in (eq. 4.2) is applied to the expressions of the first and second moments of the distribution of neutrons that slow down to thermal energy in chapter 2.2. The integrals are evaluated numerically in *MATLAB* with the code *Enrico*, described below. The code *Enrico* was written by the present author for this particular problem.

4.1.1 Description of the *Enrico* code

Enrico is written in *MATLAB*, which is a frequently used tool for scientific computing with a wide range of applications in the field of technical and engineering calculations. From the beginning, *MATLAB* was a purely mathematical tool, with particularly strong capability of dealing with matrix objects - the abbreviation *MATLAB* stands for *MATrix LABoratory*. Nowadays, *MATLAB* and the extensive family of associate toolboxes that has been developed offer high-performance in many other problems.

In the Enrico code, the second moment of the distribution of thermalized neutrons is calculated in two ways, both by the correct application of number dependent spectra and by using the average spectrum for all numbers of generated neutrons. In the expressions for the second moments computed in these two ways, $\langle \nu(\nu-1) \rangle_{correct}$ and $\langle \nu(\nu-1) \rangle_{average}$ (eq. 2.10 and 2.12, chapter 2.2), the non-leakage probability density $P(E)$ is replaced by the expression suggested by Fermi.

The buckling B^2 and the age function $\tau(E)$ are defined by reactor geometry and reactor materials in the following way:

The buckling B^2

A homogenous cylindrical reactor is used, and thus the geometrical buckling is written as

$$B^2 = \frac{\pi^2}{H^2} + \frac{2.405}{R^2}$$

(eq. 4.3)

with H and R denoting the height and the radius of the reactor [7].

The Fermi age $\tau(E)$

We have the definition of the age:

$$\tau(E) = \int_{E_{th}}^{E} \frac{l_{tr} l_s}{3\xi} \cdot \frac{dE'}{E'}$$

(eq. 4.4)

To evaluate the integral, information on l_s, l_{tr} and ξ, including their energy dependence, is required.

The scattering mean free path l_s

For a single material, $l_s = 1/\Sigma_s$ where Σ_s is the macroscopic scattering cross section. Since the core may consist of several different materials, a total Σ_s must be calculated by weighting the individual microscopic scattering cross sections with the atomic densities of each material:

$$\Sigma_s = \sum_i N_i \cdot \sigma_i$$

(eq. 4.5)

Microscopic cross section data are collected from the same source that supports the Monte Carlo code *Monaco*, see chapter 4.2.2.

The transport mean free path l_{tr}

For a single material, $l_{tr} = l_s/(1 - \overline{\cos\theta})$ where $\overline{\cos\theta}$ is the average of the cosine of the scattering angle in the elastic collision, which could be expressed

$$\overline{\cos\theta} = \frac{2}{3A}$$

(eq. 4.6)

where A stands for the mass number of the nucleus that is struck by the neutron [7]. When several different materials are involved, $\overline{\cos\theta}$ is calculated as a weighted sum of $\overline{\cos\theta}$:s, using individual macroscopic scattering cross sections as weights [1, 8]:

$$\overline{\cos\theta} = \frac{\sum_j \Sigma_{sj} \cdot (\overline{\cos\theta})_j}{\sum_j \Sigma_{sj}}$$

(eq. 4.7)

The average logarithmic energy loss per collision ξ

In [7], an expression for ξ is derived that only involves the mass number of the colliding nucleus:

$$\xi = \frac{\alpha_A \cdot \ln \alpha_A}{1 - \alpha_A} \qquad \alpha_A = \left(\frac{A-1}{A+1}\right)^2$$

(eq. 4.8)

It has been assumed that collisions are perfectly elastic.

An average ξ of a composite core is calculated by weighting the individual ξ:s with the macroscopic scattering cross sections of each material, according to [6]:

$$\xi = \frac{\sum_j \Sigma_{sj} \cdot \xi_j}{\sum_j \Sigma_{sj}}$$

(eq. 4.9)

Enrico executes all the weighted sums that are necessary to compute l_s, l_{tr} and ξ of a core that is made up of a number of materials.

The *Enrico* code requires input information on volumetric concentrations, mass numbers, molar weights and densities of each core material, and on cross section data libraries. With these data at hand, the age of the neutrons can be calculated for all energies from thermal energy up to an arbitrary limit.

The integration involved in the evaluation of the age expression in (eq. 4.4) is performed by utilization of *MATLAB*'s built-in numerical integration routines.

Calculations and output

When the age function $\tau(E)$ is determined for all energies, non-leakage probabilities $P(E)$ can be calculated, and the field is prepared for evaluation of α, (eq. 2.14). Integrals that appear in the formulae are all evaluated numerically in *MATLAB*.

The distribution of the number of spallation neutrons $p(n)$ used in this code is the one extracted from calculations with the *NMTC/JAERI97* code.

The three spectrum models described in the previous chapter are implemented in the code.
For each spectrum model, the average energy is calculated, and also the two-dimensional correlation function (eq. 2.15).

A summary of the output from the *Enrico* code is given below:

- The average energy of the source neutrons: $\bar{E}$
- The average number of source neutrons: $\bar{\nu}$

- The second moment of the number of thermalized neutrons, correctly calculated with number dependent energy spectra of the source neutrons: $\langle \nu(\nu-1) \rangle_{correct}$

- The second moment of the number of thermalized neutrons, calculated with the average spectrum of the source neutrons: $\langle \nu(\nu-1) \rangle_{average}$

- The α value $\left(\alpha = \frac{\langle \nu(\nu-1) \rangle_{correct}}{\langle \nu(\nu-1) \rangle_{average}} \right)$

- A plot of the two-dimensional correlation function.

4.1.2 Calculation cases

Two different core compositions were studied in the framework of this paper:

1. A pure ^{238}U core

2. A homogeneous core with the following volumetric proportions: 25 % uranium fuel, 50 % Pb, 25 % Fe, where the fuel composition was: 90 % ^{238}U and 10 % ^{235}U

A pure ^{238}U core is studied because it is a simple system, and the results from the calculations could easily be compared with later attempts to reproduce them. In addition, fission and neutron capture would not play a big role in a core that consists of ^{238}U only, and the calculations based on Fermi age theory, which was developed for studying slowdown through elastic scattering alone, would be more reliable.

The core composition with 50 % Pb, 25 % enriched uranium fuel and 25 % steel is an average of the compositions in various concepts that have been proposed for the design of an accelerator driven reactor. No full-scale device of this kind has yet been constructed, and the questions of core composition, core size and core geometry are still open.

For each core composition, two different geometries were used:

1. Core radius = 50 cm, Core height = 300 cm.
2. Core radius = 100 cm, Core height = 500 cm.

The *effective multiplication factor* k_{eff} was calculated for the four different reactors, using the Monte Carlo code MCNP, which gave the following results:

TABLE 1. Effective multiplication factors for the core compositions employed

	R = 50 cm, H = 300 cm	R = 100 cm, H = 500 cm
Pure ^{238}U core	$k_{eff} = 0.341$	$k_{eff} = 0.346$
Mixed core	$k_{eff} = 0.720$	$k_{eff} = 0.946$

4.1.3 Results

These are the results obtained by *Enrico* calculations:

Core composition 1: 100 % ^{238}U

TABLE 2. α-values for different reactor geometries and models of the energy distributions of the spallation neutrons for a core containing only ^{238}U

	R = 50 cm, H = 300 cm	R = 100 cm, H = 500 cm
Spectrum model	α	α
Gaussian, σ = 0.1 MeV	**1.186**	**1.064**
Maxwell	**1.173**	**1.042**
piece-wise linear	**0.964**	**0.994**

Core composition 2: 25 % fuel (90 % ^{238}U, 10 % ^{235}U)
50 % Pb
25 % Fe

TABLE 3. α-values for different reactor geometries and models of the energy distributions of the spallation neutrons for a core containing a mix of ^{238}U, ^{235}U, *Pb* and *Fe*

	R = 50 cm, H = 300 cm	R = 100 cm, H = 500 cm
Spectrum model	α	α
Gaussian, σ = 0.1 MeV	**1.083**	**1.040**
Maxwell	**1.062**	**1.016**
piece-wise linear	**0.990**	**0.998**

4.1.4 Discussion

The results of the *Enrico* calculations indicate that deviations in the second moments of the number of thermalized neutrons can be quite large when Gaussian and Maxwell distributions model the energy distribution of spallation neutrons, but significantly smaller with the piece-wise linear model. The Gaussian distribution, which imposes the strongest number dependence on the energy distribution, also gives the largest deviations.

The fact that the α values are greater than one for the Gaussian and Maxwellian distribution but less than one when the piece-wise linear model is used tells us that the second moment of the number of thermalized neutrons is overestimated by the Gaussian and Maxwellian distributions and underestimated by the piece-wise linear one, if only the

average spectrum is used to describe the energy distribution of the source neutrons. Whether α exceeds one or not is in fact determined by the correlation function, defined in eq. 2.15. To see this, rewrite the expression for α in eq. 2.14 by using eq. 2.15:

$$\alpha = \frac{\int_0^\infty \int_0^\infty P(E_1) \cdot P(E_2) \cdot (c(E_1, E_2) + \bar{\chi}(E_1) \cdot \bar{\chi}(E_2)) dE_1 dE_2}{\int_0^\infty \int_0^\infty P(E_1) \cdot P(E_2) \cdot \bar{\chi}(E_1) \cdot \bar{\chi}(E_2) dE_1 dE_2} = \ldots$$

$$\ldots = \frac{\int_0^\infty \int_0^\infty P(E_1) \cdot P(E_2) \cdot \bar{\chi}(E_1) \cdot \bar{\chi}(E_2) dE_1 dE_2 + \int_0^\infty \int_0^\infty P(E_1) \cdot P(E_2) \cdot c(E_1, E_2) dE_1 dE_2}{\int_0^\infty \int_0^\infty P(E_1) \cdot P(E_2) \cdot \bar{\chi}(E_1) \cdot \bar{\chi}(E_2) dE_1 dE_2} = \ldots$$

$$\ldots = 1 + \frac{\int_0^\infty \int_0^\infty P(E_1) \cdot P(E_2) \cdot c(E_1, E_2) dE_1 dE_2}{\left(\int_0^\infty P(E) \cdot \bar{\chi}(E) dE \right)^2}$$

(eq. 4.10)

The denominator in the last term is always greater than zero, so the sign of the term is determined exclusively by the integral over the correlation function $c(E_1, E_2)$, weighted by the non-leakage probability $P(E)$. The sign of this integral can be estimated by studying the characteristics of the correlation function belonging to each spectrum model.

Take for example the correlation function of the Maxwell distribution, plotted in Figure 10. This function is greater than zero in the low energy region, where the non-leakage probability is large, and thus, the weighted integral is given a large positive contribution. Therefore, the total integral could be expected to be greater than zero for this correlation function and we would have $\alpha > 1$.

On the other hand, it is clear from Figure 12 that the correlation function belonging to the piece-wise linear model is negative at low energies, suggesting α to take on a value less than 1. The correctness of this hypothesis is indeed confirmed by the results in tables 2 and 3.

As one might expect from the expression for the non-leakage probability employed here, where the probability increases exponentially with the geometrical buckling, the size of the system has a strong influence on the α value. The smaller the system, the more the α value deviates from one.

When the two core compositions are compared, one notices that deviations are reduced in a mixed core of enriched uranium fuel, lead and steel, compared to a pure uranium core.

4.2 Monte Carlo calculations

Along with the analytical calculations of the second moment that were presented in the previous chapter, a completely different technique has been employed to estimate the significance of the energy distributions of the spallation neutrons on the second moments. *Monte Carlo calculations* are the methods referred to, and before diving into the details of the code that has been developed with this technique, it might be useful to sketch out its main principles.

4.2.1 Monte Carlo principles

Monte Carlo calculations have proved to be an efficient tool in simulation of physical systems, especially those systems in which the processes involved are of statistical nature.

Unlike the closed form of well-defined equations that usually result from analytic treatments of a problem in physics or mathematics, the idea with the Monte Carlo approach is to simulate the actual processes for a large number of times and then to extract the results from the statistics of the calculated variables.

A simple and illustrating example of how this could be done is comparing two ways of treating the problem of coin-tossing. If one side of a coin is given the value 1 and the other 0, analytical calculations immediately determine the mean value of the tossing to be 0.5, at least if both sides land with its face up with equal probability. With Monte Carlo methods, the idea would instead be to perform a large number of random simulations of the coin-tossing process, where the outcome of the two possible events both have probability 0.5. As the number of simulations increase, the mean value converges to 0.5, which is concluded to be the true mean value of the tossing.

Several other examples could be given with close connection to gambling and game problems, and this is of course from which the name of the methodology origins.

Since the number of random samplings needed to achieve sufficient convergence may be very large, Monte Carlo methods are usually time-consuming and demand powerful computer facilities. Although the basic ideas of Monte Carlo methods are quite old, it is therefore not until the appearance of high-performance computers they have been possible to utilize.

The example with the tossing of a coin does not show the advantages of Monte Carlo methods, since the result was more easily calculated analytically, and furthermore, their time-consuming features and high requirements of computer power do not sound very appealing. However, the advantages of the Monte Carlo technique can be overwhelming. In fact, in problems where the geometry of a problem is difficult and where the relations between physical quantities are non-analytical, Monte Carlo calculations are sometimes the only way to obtain a solution.

In reactor physics, Monte Carlo methods have been used to simulate the neutron transport and the reactions in nuclear reactors - an excellent application, since the processes involved are of purely random nature. The common analytic treatment of the neutronics of a nuclear reactor involves the formulation of the *Boltzmann Transport Equation*,

which is often very hard to solve. Moreover, this equation only holds for average values. When fluctuations are to be calculated, it is necessary to use *master equations* which are generally even more difficult to solve [9].

The Monte Carlo approach offers a less cumbersome alternative. Individual neutrons are traced, and what reactions they undergo is decided by random sampling from a probability distribution that is based on reaction cross sections. Each step of the calculation are then very simple, and the whole calculation procedure could be thought of as a succession of such basic calculation steps. Of course, the large number of neutrons in a nuclear system makes the number of required calculations huge, but since each step are very simple, a powerful computer could still manage to do it.

4.2.2 Description of the Monte Carlo code *Monaco*

The code that has been constructed to simulate the transport of neutrons in a a reactor using a Monte Carlo approach for the calculations, is written in *MATLAB* and has been given the name *Monaco*, the country in which Monte Carlo is the capital.

Spallation neutrons are generated in the spallation model elaborated earlier (chapter 3.2), the neutrons are injected into a nuclear reactor core, and the subsequent neutron reactions in the core are computed by tracing the individual neutrons. The procedure is repeated for a large number of spallation events, statistical variables are calculated again and again, until the mean value and the covariance converge.

The diagram below gives a brief description of the code structure.

begin
- Define control variables and core data
- Initialize calculation data lists

for each spallation event
- Generate a list of spallation neutrons

for each neutron in the list, until the list is empty
- Calculate cross sections for different reactions, depending on the neutron energy
- Choose the next reaction by random sampling, and determine the distance to the position at which the reaction takes place
- Move the neutron this distance in the direction of its velocity vector
- Check if the moved neutron is still inside the core
- Depending on the event, generate new neutrons to be added to the neutron list, or remove the neutron from the list.
- Update calculation data lists

end loop
- Update calculation data lists

end loop
end

The most important parts of the code are described in greater detail in the following.

Definition of control variables

Before starting calculations with the *Monaco* code, a set of parameters specifying options and modes of the execution must be defined. For example, the number of spallation events in each case must be specified. This number should be large enough to enable sufficient convergence of the first and second moments of the quantities considered.

Definition of core data

Nuclear masses, molar weights and densities of the fuel and other core materials are listed in the code, and the volumetric composition of the core must be specified by the user. The code treats the core as a perfectly homogenous one, with each material appearing in volume ratios that are given as input.

The following core materials, apart from the fuel, can be included in the core:

Iron (^{56}Fe), lead (^{208}Pb), bismuth (^{209}Bi), sodium (^{23}Na), oxygen (^{16}O)

The composition of the fuel must also be specified, and the molar fraction of each component should be given. As with the rest of the core, the fuel is treated homogeneously, and it could be regarded as if it was evenly spread over the whole core volume.

These materials are available for fuel composition:

^{238}U, ^{235}U, ^{239}Pu, ^{16}O

A simple cylindrical geometry is used for the homogenous core. Thus, only the core radius and core height need to be defined in order to fully specify the core geometry.

The target, on which a high-energy proton impinges and in which spallation neutrons are generated, can be modelled either by a point-like neutron source or a cylindrical source. If a cylindrical target is used, the size of the target must also be specified.

The only target material that can be used is ^{208}Pb.

Generation of spallation neutrons

In the *Monaco* code, six numbers define the state of each neutron:

- three spatial coordinates to define the position of the neutron
- the speed of the neutron
- two angles to define the direction of the velocity vector

neutron = [x y z speed φ θ]

The z-axis is along the symmetry axis of the cylindrical core and z = 0 is the point where the proton beam enters the reactor. θ is the polar angle that the velocity vector makes with the z-axis, and φ is the azimuthal angle that the projection of the velocity vector in the x-y-plane makes with the x-axis.

A list of spallation neutrons, each of them specified by the six numbers, is generated in a number of steps:

1. Pick a number of spallation neutrons n from the probability distribution $p(n)$.
   The distribution used is the one that was extracted from *NMTC/JAERI97*.

2. Determine the position of the spallation event.
   There are two options for the spatial distribution of the spallation neutrons:

   a) a cylindrical target
   b) a point-like target

   If a cylindrical target is used, the position of the spallation reaction is randomly sampled with equal probability within the target. The target is included as a part of the core, and neutron transport inside of the target (elastic scattering and capture) is simulated.

For each of the n neutrons:

3. Pick a spallation neutron energy by random sampling from probability distributions that model the energy spectra of the spallation neutrons.
   The probability distributions can be any of the three models described in chapter 3.4, and one must indicate if number dependent spectra or the average spectrum is to be used.

   The speed v of the neutron is calculated from the kinetic energy E by using the relativistic formula:

$$v = c \cdot \sqrt{1 - \frac{1}{\left(1 + \frac{E}{mc^2}\right)^2}} \qquad \text{(eq. 4.11)}$$

   where c is the speed of light.

4. Determine the direction of the velocity vector.
   Two options are available for the distribution of spallation neutron velocity directions:

   a) ejection of spallation neutrons is isotropic
   b) neutrons ejected in the forward direction is favoured

   If option b) is used, one half of the neutrons are generated with a positive velocity component in the direction of the incoming particle, i.e. they move forward, and the other half of the neutrons are isotropically generated.

Random sampling methods

When sampling values are to be picked from probability distributions, various techniques can be employed. But regardless of what sampling method is used, it always includes somewhere the generation of a random number. For the purposes of random samplings in the *Monaco* code, *MATLAB*'s built-in random number generator has been used. This generator can generate floating point numbers from a uniform distribution on the interval [0, 1].

Here is a presentation of the three different sampling techniques that are used in *Monaco*:

1. Straightforward sampling by probability function inversion

The most elegant and often most efficient sampling method is to use an inversion of the probability function that takes a random number as argument. This method demands a simple analytical expression for the probability function. For example, when the distance to the next reaction of a neutron is determined, the expression for the probability $p(x)$ of a reaction to occur at a distance x from a certain point is

$$p(x) = \frac{1}{\Sigma_{tot}} \cdot e^{-\Sigma_{tot}x} \qquad \text{(eq. 4.12)}$$

where Σ_{tot} is the total macroscopic cross section. From this equation a formula can be derived that makes picking random distance values x from this exponential distribution very simple:

$$x = -\frac{1}{\Sigma_{tot}} \ln r \qquad \text{(eq. 4.13)}$$

where r is a value that has been picked from a uniform distribution between 0 and 1 [10].

Probability distributions from which values have been picked by analytical expressions in the *Monaco* code are:

- Number dependent, piece-wise linear distribution of spallation neutron energy
- Probability distribution of the distance to the next reaction

2. Rejection methods

When continous probability distributions cannot be given as an analytical formula like in (eq. 4.11), it is impossible to derive exact analytical formulas for straightforward samplings, and the problems must be attacked in some other way. In some of these cases, *Monaco* apply rejection techniques for the sampling procedure, and it is done as follows:

- First, a number x_1 is picked randomly from the interval on which the probability distribution $p(x)$ is defined.

- Then, a number y_1 is picked that lies between the lowest and the highest value of the probability function, this too with equal probability on the whole interval.

- The probability function is then evaluated at point x_1, and this value, $p(x_1)$, is compared to y_1. If $y_1 < p(x_1)$, the point (x_1, y_1) lies below the graph of the probability function and x_1 is accepted as the chosen value. If not, the point (x_1, y_1) is rejected, and a new pair of values (x_2, y_2) is picked, y_2 is compared to $p(x_2)$, and so on.

The whole procedure could be thought of as a blind person throwing tomatoes on a wall, the area under the probability function being the target. The tomatoes are thrown in random directions, and if any of them hits the target area, they are registered. See Figure 13 below.

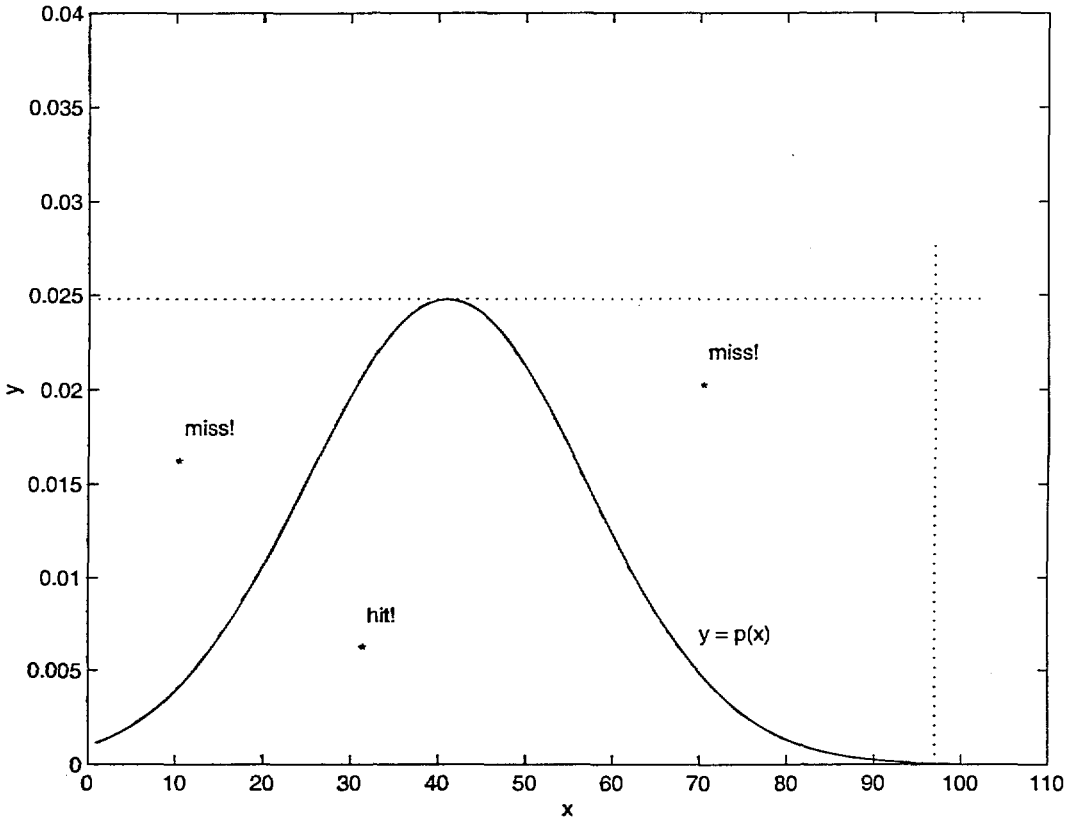

FIGURE 13. Illustration of the principles of random sampling with rejection methods.

In the *Monaco* code, rejection methods are used when values are chosen from any of the following probability distributions:

- Number dependent Maxwell distribution of spallation neutron energy
- Average Maxwell distribution of spallation neutron energy
- Number dependent Gaussian distribution of spallation neutron energy

- Average Gaussian distribution of spallation neutron energy
- The number of spallation neutrons
- The energy of the neutrons generated in fission reactions

3. if-*statements for simple discrete distributions*

The number of neutrons that are generated in fission is described by a discrete probability function. Since the maximum number of fission neutrons is only at about six, it is sufficient to pick a random number between 0 and 1, and then comparing this number with the accumulated probabilities for each fission neutron number, in a sequence of *if*-statements.

Picking the next reaction and the distance to it

To determine what reaction will be induced by the neutron in question, a random picking procedure is employed, with the probability for reaction i to occur being denoted p_i, defined as

$$p_i = \frac{\Sigma_i}{\Sigma_{tot}}$$

(eq. 4.14)

where Σ_i is the macroscopic cross section for reaction i, and Σ_{tot} is the total macroscopic cross section.

The following reactions are treated in the code:

1. Elastic scattering
2. Fission
3. Neutron capture

All other reactions, such as inelastic scattering, secondary spallation and n-p-reactions that occur at high energies are not considered in the code. This limits the validity of the code, especially since high-energy neutrons are dealt with.

When the next reaction has been determined, the distance to the position at which the reaction takes place is determined by random sampling from the probability distribution $p(x)$:

$$p(x) = \frac{1}{\Sigma_{tot}} \cdot e^{-\Sigma_{tot} x}$$

(eq. 4.15)

Fission reactions

If the reaction that has been picked is fission, the following steps are executed:

1. Remove the neutron that caused fission from the neutron list

2. Pick a number of fission neutrons from a fission neutron number probability distribution.
   Although both thermal and fast fission of three fissile nuclides (^{235}U, ^{238}U and ^{239}Pu) are treated, the number distribution that is used is based on data for thermal fission of ^{235}U The same distribution is used regardless of what nuclide undergoes fission and regardless of the neutron energy, and this is of course a simplification.

3. For each fission neutron, assign to it three space coordinates (the space coordinates of the position of the fission event), a speed (converted from kinetic energy), and two angles that specify the direction of the velocity vector.
   Energy is randomly sampled from a probability distribution that corresponds to the fission spectrum of ^{235}U by thermal neutrons, independent of what nuclide is fissioned and regardless of the energy of the incoming neutron - another simplification. Fission is assumed to be isotropic, i.e. all directions of the velocity vector of a fission neutron are picked with equal probability.

4. Add the new neutrons to the neutron list

Scattering reactions

There are two options for treating the scattering process in the code:

a) Isotropic elastic scattering
b) Non-isotropic elastic scattering

In case a) energy losses of the colliding neutron are calculated in accordance with formulae from [7], but all directions of the outgoing neutron are considered to be equally probable. In case b) angular distributions of the outgoing neutron derived in [7] are employed, which yields a slightly more accurate simulation of the scattering process.

In order to simplify the problem, inelastic scattering is not considered here. Ignoring the inelastic scattering is a quite heavy simplification since it is an important process, not only in high-energy systems like the ones treated here, but also in thermal reactors.

Neutron absorption, thermalization and leakage

Neutrons that are absorbed by the fuel or any other core material, and neutrons that leak out from the system, or reach a certain minimum energy level, are removed from the neutron list. The code keeps counting how many neutrons have leaked out, how many neutrons have been captured in each material etc., but the position and velocity of any neutron that leaves the system is not recorded.

Cross section data

The cross sections that are used by *Monaco* are based on cross section models from [11]. These cross section models are simplifications of experimentally measured cross sections, covering the energy interval 0.001 eV - 20 MeV. Since for the time being, cross section data for neutron energies above 20 MeV are not available for a large number of nuclides, including ^{235}U and ^{238}U, assumptions must be made about the cross sections in this energy region. In the *Monaco* cross section model, cross section data have been extrapolated in a very simple way, namely by assigning the cross section value at 20 MeV to all higher energies.

The cross section library contains data for the following cross sections:

^{238}U elastic scattering cross section
^{238}U capture cross section
^{238}U fission cross section
^{235}U elastic scattering cross section
^{235}U capture cross section
^{235}U fission cross section
^{239}Pu elastic scattering cross section
^{239}Pu capture cross section
^{239}Pu fission cross section
^{208}Pb elastic scattering cross section
^{208}Pb capture cross section
^{209}Bi elastic scattering cross section
^{209}Bi capture cross section
^{16}O elastic scattering cross section
^{16}O capture cross section
^{56}Fe elastic scattering cross section
^{56}Fe capture cross section
^{23}Na elastic scattering cross section
^{23}Na capture cross section

The listed reactions were chosen since they are considered to be the dominant ones in neutron transport inside the core, but the cross section library could easily be extended to include other reactions.

The macroscopic cross section Σ_{ij} for the reaction i in material j is calculated from microscopic cross sections σ_{ij} and atomic densities N_j in the ordinary way:

$$\Sigma_{ij} = \sigma_{ij} \cdot N_j \qquad \text{(eq. 4.16)}$$

where

$$N_j = \frac{\rho_j \cdot N_A}{M_j} \qquad \text{(eq. 4.17)}$$

ρ_j denoting the density of material j, M_j the molar weight, and N_A being the Avogadro number (= $6.022*10^{23}$).

Program output

When *Monaco* calculations are terminated, a number of data arrays have been saved. They contain information about the statistics of the nuclear reactions that have taken place in the core due to the release of the initial spallation neutrons.
Each data array is N elements long, where N is the number of spallations, and the value of each element denotes how many ^{235}U fissions were caused by this particular swarm of spallation neutrons, how many captures occurred in ^{238}U due to the same spallation, how many neutrons leaked out, etc.

The following quantities are stored in data arrays for each spallation:

- The number of spallation neutrons
- The number of captures in ^{238}U, ^{235}U, ^{239}Pu, ^{208}Pb, ^{209}Bi, ^{16}O, ^{56}Fe, ^{23}Na
- The number of elastic collisions in ^{238}U, ^{235}U, ^{239}Pu, ^{208}Pb, ^{209}Bi, ^{16}O, ^{56}Fe, ^{23}Na
- The number of fissions in ^{238}U, ^{235}U, ^{239}Pu
- The number of out-leaked neutrons
- The number of thermalized neutrons
- The execution times

By utilizing *MATLAB*'s plot routines, some of the computed data are continuously plotted on the screen during the calculation. For example, the mean value and the covariance of the number of fissions in ^{238}U is plotted for each spallation, which makes it possible to follow the convergence of this quantity.

Code limitations

Any observant reader can notice from the above code description that several simplifications and assumptions has been necessary in order to make the problem possible to treat with a model that is not too complex. This will of course impose limits on the validity of the code, and on the accuracy of the results calculated. However, the main object of this work has not been to provide exact results, but to show what the approximate size of the variables in question is, to indicate the influence of different spallation neutron spectra on the second moment. Anyway, it is important to point out the major sources of error in the code that are caused by simplifications of the physical model on which the code is mounted. Improvements of the model can hopefully yield more accurate and detailed results in future treatments of the problem.

Nuclear reactions

Inelastic neutron scattering, (n,p)-reactions, secondary spallations and many other are left out of the *Monaco* code, even if they do play an important role in neutron transport, especially at energies in the MeV region.

The transport of and the reactions induced by protons, pions and α-particles are not taken into account, although their presence at high-energy nuclear reactions undoubtedly affects the system.

Cross section data

The cross sections that were available at the time for the construction of the *Monaco* code was only supported by experimental data up to 20 MeV, and for higher energies it was necessary to make straight-line approximations. This will obviously cause a deterioration of the correctness of the calculated results.

Core geometry

The core was assumed to be cylindrical and perfectly homogenous, with no reflector, which must be regarded as a serious simplification of any actual accelerator driven system.

Core composition

Only a few different types of material are included in the core model, leaving out the wide spectrum of fission products and construction materials that would most probably appear in any accelerator driven system.

4.2.3 Calculation cases

The same cases that were analysed with the Enrico code were also studied with Monaco, i.e.:

Two different core compositions:

1. A pure ^{238}U core

2. A homogenous core with the following volumetric proportions:

25 % uranium fuel
50 % Pb
25 % Fe

where the fuel composition was the following:

90 % ^{238}U
10 % ^{235}U

Two different core geometries:

1. Core radius = 50 cm, Core height = 300 cm.
2. Core radius = 100 cm, Core height = 500 cm.

4.2.4 Results

Results from *Monaco* calculations are presented as ratios between second moments calculated correctly (with number dependent energy spectra for the spallation neutrons) and in an average manner (using only the average energy spectrum). Different from the calculations performed with the *Enrico* code in chapter 4. 1, we will not focus on the number of thermalized neutrons, but instead on the number of fissions and elastic scatterings in ^{238}U, and on the number of out-leaked neutrons. The results are presented in Tables 4 to 7 below. Each figure denotes a ratio between the second moments (covariances) calculated in the two different ways, e.g. in the case of fissions in ^{238}U:

$$\frac{\text{covariance of the number of } ^{238}U \text{ fissions (number dependent energy spectra)}}{\text{covariance of the number of } ^{238}U \text{ fissions (average energy spectra)}}$$

The numerical error attached to these results due to the fact that only a finite number of spallation events have been used are estimated to be less than 2 %.

Core composition 1:

100 % ^{238}U

TABLE 4. Covariance ratios for a pure uranium core, R = 50 cm, H = 300 cm.

Core dimensions: R = 50 cm, H = 300 cm			
Spectrum model	^{238}U fissions	^{238}U scatterings	out-leaked neutrons
Gaussian	**0.76**	**0.82**	**0.83**
Maxwell	**0.75**	**0.80**	**0.82**
piece-wise linear	**1.16**	**1.07**	**1.11**

TABLE 5. Covariance ratios for a pure uranium core, R = 100 cm, H = 500 cm.

Core dimensions: R = 100 cm, H = 500 cm			
Spectrum model	^{238}U fissions	^{238}U scatterings	out-leaked neutrons
Gaussian	**0.80**	**0.82**	**0.84**
Maxwell	**0.79**	**0.81**	**0.83**
piece-wise linear	**1.12**	**1.08**	**1.10**

Core composition 2:

25 % fuel (90 % ^{238}U, 10 % ^{235}U)
50 % Pb
25 % Fe

TABLE 6. Covariance ratios for a core containing a mix of ^{238}U, ^{235}U, Pb and Fe, R = 50 cm, H = 300 cm.

Core dimensions: R = 50 cm, H = 300 cm			
Spectrum model	^{238}U fissions	^{238}U scatterings	out-leaked neutrons
Gaussian	**0.71**	**0.86**	**0.86**
Maxwell	**0.72**	**0.83**	**0.84**
piece-wise linear	**1.12**	**0.98**	**1.05**

TABLE 7. Covariance ratios for a core containing a mix of ^{238}U, ^{235}U, Pb and Fe, R = 100 cm, H = 500 cm.

Core dimensions: R = 100 cm, H = 500 cm			
Spectrum model	^{238}U fissions	^{238}U scatterings	out-leaked neutrons
Gaussian	**0.71**	**0.84**	**0.85**
Maxwell	**0.71**	**0.84**	**0.81**
piece-wise linear	**1.12**	**0.99**	**1.04**

4.2.5 Discussion

The following conclusions can be drawn from the results of *Monaco* calculations:

If the energy distributions associated to different neutron numbers show strong individual variance, which is true in the case of Gaussian and Maxwell spectrum models, the difference in calculated second moments can be significant, up to 30 %. These two spectrum models give similar results in all the cases studied.

But also for spectra generated by *NMTC/JAERI97*, which is probably the most realistic model of the neutron energy distributions, deviations are still significant, with a maximum of 16 % for the number of ^{238}U fissions in the smallest core geometry. Deviations that follow from this spectrum model are generally smaller than what is predicted by the two more artificial Gaussian and Maxwellian distributions, but they can by no means be neglected.

With the "realistic" spectra, the second moment of the number of ^{238}U fissions, ^{238}U fissions and out-leaked neutrons are underestimated, if only the average spectrum is

used to determine the distribution of the energy of the spallation neutrons. This information is given from the fact that the second moment ratios are greater than one, which is true for the case with piece-wise linear spectrum models. The opposite is true for Gaussian and Maxwellian spectrum models, i.e. second moments are overestimated.

This is thus different from the case with thermalized neutrons, which was treated by Fermi age theory in chapter 4.1. However, no contradictions between the *Enrico* and *Monaco* results exist in this respect - we just have to remember that different variables are calculated by the two codes. *Enrico* calculates the second moment of thermalized neutrons, and α-values less than zero for the piece-wise linear model were expected from (eq. 4.10) and the correlation function in Figure 12. The *Monaco* code, on the other hand, deals with fissions, elastic scatterings and out-leaked neutrons and no analytical expressions are at hand to allow a priori estimates of the second moment ratios.

Nevertheless, we take confidence from noting that the ratio of the second moment of out-leaked neutrons is greater than one in the case of piece-wise linear spectra. This is opposite to the calculated α-values (referring to thermalized neutrons, i.e. the neutrons that *do not leak out*) with the same spectrum model, but it could be reproduced by the same equations. By replacing the non-leakage probability $P(E)$ with the leakage probability $1-P(E)$ in (eq. 4.10), the ratio between correctly and "averagely" calculated second moments of *out-leaked neutrons* would be calculated. Following the discussion in chapter 4.1.4, the value of this ratio is then expected to be greater than one when the piece-wise linear distributions are used, and this was also confirmed by running the *Enrico* code with the above modification (replacing $P(E)$ with $1-P(E)$).

The size of the system does not appear to have any considerable effect on the second moment ratios when Monte Carlo methods are used. Only a slight tendency of ratio values converging to 1 when core dimensions increase can be observed.

In the second core composition, where the effective multiplication factor is higher (k_{eff} = 0.72 and 0.95) the errors in estimating the second moment of the number of fissions are somewhat larger.

5. Conclusions and remarks

The results from the *Enrico* and *Monaco* calculations shows that the results from second moment calculations can be significantly different if a number dependent model of the energy distributions of spallation neutrons is used. This indicates that in simulating a real accelerator driven system including a spallation process, an average energy distribution of the spallation neutrons would not be sufficient when second moments are to be calculated. However, some remarks are in order.

Any simulation aiming at predicting the neutron statistics of an accelerator driven system in greater detail and with higher accuracy than in this work would inevitably include a thick target model, correctly simulating the high-energy reactions that takes place in the target. The processes involved in the neutron transport inside the target will decrease

significantly the differences between the energy distributions of various neutron groups, reducing the significance of number dependent energy spectra. Therefore, there are reasons to believe that the error we make by not including the number dependence but using only the average spectrum in second moment calculations of a real system is smaller.

On the other hand, the models that were used in the codes Enrico and Monaco do not claim to be the most accurate and realistic ones at hand. By including important high-energy reactions, proper cross section data, etc., deviations might increase or decrease, it is difficult to tell which. However, the fact that a divergence can be detected informs us about the hazard of not taking the problem seriously enough, and suggests that we keep paying attention to it.

6. Acknowledgements

A number of persons helped me in many different ways to complete this thesis, and to these people I am very grateful.

First of all, I owe Prof. Shiroya and his collaborators at *Kyoto University Research Reactor Institute (KURRI)* many thanks for their boundless hospitality and assistance during my stay at the institute in the summer of 1999.

Dr. D. Hilscher at *Hahn-Meitner-Institut* in Berlin, Ph. D. Jan Wallenius at *KTH* in Stockholm also contributed to this work by their valuable comments and kindful answers to the numerous questions I have asked them.

The staff at the department of reactor physics at Chalmers University of Technology, whose superb support in technical as well as intellectual matters have made my work easier, are also objects of my gratefulness.

With extra warmth and respect, I would like to thank *Svensk Kärnbränslehantering AB* for their financial support. Without their generous funding, this project could never have been carried out to the same extent.

Finally, I would like to thank my supervisor Prof. Imre Pázsit for his guidance and encouragement throughout the six month I worked on this thesis. Discussing the problems connected to the subject of my work with him was great help to me, and it brought about a welcome expansion of my knowledge of reactor physics.

7. References

[1] Prof. I. Pázsit, Department of reactor physics, CTH, Göteborg, personal communication (June - November 1999)

[2] I. Pázsit, N-G Sjöstrand and V. Fhager, *On the significance of the distribution of source neutrons in spallation.* To be submitted to Nuclear Instrument Methods (2000)

[3] Dr. D. Hilscher, Hahn-Meitner-Institut, personal communication (June - July 1999)

[4] H. Takada, N. Yoshizawa, K. Kosako and K. Ishibashi, *JAERI-DATA/Code 98-005, "An upgraded version of the nucleon meson transport code: NMTC/ JAERI97"*, Japan Atomic Energy Research Institute (1998)

[5] D. Hilscher *et al.*, Nucl. Instr. Meth. A **414**, 100 (1998)

[6] Lamarsh, *Introduction to nuclear reactor theory*, ch. 7, p.225, eq.7-33. Addison-Wesley (1966)

[7] N-G Sjöstrand, *Reaktorfysik*, CTH, Göteborg (1998)

[8] G. I. Bell and S. Glasstone, *Nuclear Reactor Theory*, ch. 1.1b, p. 10 and ch. 2.6, p. 104 Krieger Publ. Co. (1985)

[9] M. M. R. Williams, *Random processes in Nuclear Reactors.* Pergamon press (1973)

[10] E.D. Cashwell and C.J. Everett, *A practical manual on the Monte Carlo Method for random walk problems,* Los Alamos Scientific Laboratory, University of California. Pergamon Press (1959).

[11] K. SHIBATA, T. NAKAGAWA, H. SUGANO and H. KAWASAKI, *JAERI-Data/Code 97-003 (Part I and II), "Curves and tables of neutron cross sections in JENDL-3.2" (1998)*